The devil's in the disequilibrium: sensitivity of ocean carbon storage to climate state and iron fertilization in a general circulation model
Sarah Eggleston and Eric D. Galbraith
bg-2017-328

Response: Reviewer 1

This paper describes some 44 simulation scenarios with the GFDL climate model in order to understand which processes might be responsible for the glacial CO2 drawdown, which is observed in the ice core data.

The paper makes an separation of DIC into the soft issue pump, the carbonate pump, and saturation and disequilibrium, and might in principle be worth publishing. However, the form of presentation needs some fundamental rework for various reasons, which are find below. I find both the representation of the text and of the results in the figure very sloppy and full of not very detailed descriptions.

1. Main issue: As already indicated by the title of the paper the disequilibrium component of DIC is the part of the carbon fluxes which seemed to be of major relevance, but which seemed to have been neglected in previous papers. Disequilibrium DIC ist the difference between saturated DIC (surface ocean DIC in equilibrium with the atmosphere, here defined by constant 270 ppm) and actual DIC. Marine carbon uptake is slowed down by the marine carbonate chemistry, because DIC for present surface ocean conditions is found as 1% CO2, 90% HCO3 and and 9% CO3, but only the 1% CO2 can exchange with the atmosphere. My understanding of the disequilibrium DIC is therefore, that it represents a different way of saying, that oceanic carbon uptake is restricted by marine carbon chemistry. For example, a change in atm CO2 by 10% leads only to a change in DIC of about 1%. This effect of the chemistry is summarized by the Revelle or buffer factor R = (ΔCO2/CO2)/(ΔDIC/DIC) which is around 10, but various between 8 and 15 (e.g. Sabine et al., 2004, Science). Since full carbon cycle models all include the relevant carbonate chemistry, this effect is always included, and I am missing a connection of the newly analysed disequilibrium component of DIC with this issues. Maybe the disequilibrium DIC is not that new at all.

Thank you for the comment, which has indicated to us that the terms were not sufficiently described in the initial submission. We will elaborate on the discussion of DIC(dis) in the introduction of the text to clarify what it represents, and we plan to add a new figure to illustrate the concepts more clearly. In short, the disequilibrium component is indeed related to the carbonate chemistry, which slows the air-sea exchange as described, but it is also a function of biological uptake, ocean circulation, and gas exchange. It can be seen as the net result of all non-equilibrium processes on the DIC concentration within the surface layer.
It is also absolutely true that the disequilibrium effect is included in all full carbon cycle models (though, as pointed out on page 3 in lines 18-20, this component is by definition excluded from models when air-sea gas exchange is assumed to be infinitely fast). The purpose in recognizing it as an explicitly defined component of carbon storage is for understanding the underlying mechanisms. For example, in studying the glacial-interglacial change, the focus is generally on the importance of the saturation and soft tissue "pumps"

(e.g., Archer et al., 2000; Sigman and Boyle, 2000). We note that Ödalen et al. (Biogeosciences Discussions, 2017) use a similar approach, with a similar motivation.

2. Therefore, I have the feeling, the paper is lost in details, but misses more strength on a red line.

Thank you for the suggestion to highlight the take-home messages more clearly; we intend to make this a central goal of the revision.

3. I also believe the scenario definition with fixed and constant CO2 at 270 ppm is a major drawback in the value of the paper, since it implies that all quantifications of the fluxes have to be treaded very carefully: They have to be wrong, since the gas exchange of CO2 heavily depends on the pressure gradient in CO2 between atmosphere and ocean.

The choice to hold CO_2 constant at 270 ppm will indeed have an effect on DIC(dis). And of course, as George Box famously noted, all models (including this one) are wrong. However, as discussed on page 11 in lines 22-25, the atmospheric CO_2 acts primarily on the saturation concentration, while the effect on the disequilibrium fraction is expected to be small. The "minor, non-linear effects" here refer to the fact that air-sea gas exchange is itself a function of DIC(dis), as one term in the calculation of the piston velocity is the departure from equilibrium between the atmosphere and surface ocean with respect to CO_2 (using an atmospheric value of 270 ppm), as the reviewer has asserted. We recognize that this is an important point to address in more detail, and we will therefore provide a short quantitative estimate of the magnitude of this effect, along with additional clarification earlier in the paper (page 6, section 4: Discussion).

In addition to the fact that the effect is likely to be small, we note that the fact that the carbon cycle is equilibrated with 270 ppm in all cases helps to provide a cleaner comparison between simulations. The carbon cycle has many moving parts, and by holding the atmospheric CO_2 constant we provide a simpler picture of mechanistic differences. We would note that the value of the disequilibrium component will also depend on the base state of the soft tissue pump strength, ocean circulation, and alkalinity distribution, none of which are perfectly simulated by any model that we are aware of. Our work is not meant to be a definitive quantification of the disequilibrium component, rather, we hope to illustrate its conceptual importance (which has been overlooked) and show the basic controlling mechanisms.

4. The authors have chosen to keep atmospheric CO2 fixed, so they calculate changes in oceanic DIC only as a function of prescribed CO2 (always 270 ppm), which ignores dynamic aspects of the gas exchange, that largely depend on the surface ocean-atmospheric difference in pCO2. This is a significant simplication, which reduces the significance of the quantification of the process separation a lot. It implies, that atmospheric CO2 concentration is not a dynamic part of the carbon cycle analysis anymore. CO2 is nevertheless varied, but only to generate different background climatologies, implying only the radiative forcing of CO2 is used here. I therefind find the description of all scenarios and results highly confusing, they should not be defined by the prescribed atm CO2 value, because this is not considered in the carbon cycle change, but by the resulting global annual mean surface temperature changes, ΔT. I therefore expect, that the authors, (i) calculate ΔT, probably with respect to their control simulation (probably the one with CO2 = 270 ppm), and (ii) use ΔT when describing the scenarios, in the text, in Table 1, and in the Figures (e.g. x axis of Fig 1, 4). Since changes in

obliquity, precession, and land ice sheet might also change ΔT, they might also be more specific and call this ΔTCO2, but they might then also analyse the temperature change related to these other processes. If they then plot results in Fig 1 as function of Delta T, a lot of the various scenarios with similar CO2, but different other boundary conditions might then separte in ΔT, and might be easier to be identified. Right now Fig 1 is an mess, with various symbols plotted on top of each other. If thss step does not improve figure 1, the authors might also consider to plot Fig 1 as bar charts, where different scenarios by definition are plotted NEXT and not ON TOP of each other.

Thank you for the suggestion; we can see that the radiative-CO_2 labeling was a major source of confusion for both reviewers, given that it is independent of the CO_2 used for air-sea exchange. We will relabel the axes on these plots in terms of the associated change in mean surface air temperature (ΔT). We also appreciate the suggestion to alter the plot style, but substituting a bar plot for figure 1 (as in figure 2) would reduce the amount of information that we are able to convey by eliminating the x-axis and thereby the depiction of the average DIC concentration as a function of ΔT, so we would prefer to retain this plot style, which is more easily legible when plotted vs. temperature.

5. Anomalies on mean ocean DIC are analysed given in µmol/kg. However, I would find it much more helpful, if the amount of carbon taken up by the ocean would be given in terms of PgC (= GtC), which should be transferable easily (if the mean density of water and the volume of the ocean are known). Maybe, if the authors insist on their view on the system (µmol/kg), they might simply add a 2nd y-label (right-handside) with PgC. This would help a lot, since it is not clear to me, if the setup of the climate model in the LGM mode (more land ice) would also imply less ocean volume, which would directly affect the concentration of DIC in µmol/kg, but not total amount ocean C in PgC. The discussion how much a change in DIC would change atm CO2 (Discussion, page 6) can be simplified a lot by stading the change in oceanic DIC in PgC.

Thank you for the suggestion. We will add a second y-axis indicating the change in DIC in PgC. The range of the changes in the ocean volume across the different simulations is less than 0.5%, so the changes in DIC concentration and oceanic C inventory are approximately proportional.

6. In the text various times a change in carbon due to a change in ocean circulation is seen (e.g. page 5, line 26, line 29, page 6, line 2), however, the ocean circulation state is never described in the draft. The reader does not know which of the scenarios has a slower ocean overturning. If this relationship should be kept in the text, some further details (ocean circulation analysis) is needed. My impression is, this might be found in the draft Galbraith + de Lauvergne (submitted), but this is not accessible. So, either the resubmission of this paper has to wait for the other paper, or some of these analysis need to be repeated here.

Indeed, this is a key aspect of the manuscript submitted by Galbraith and de Lavergne. Because this is a journal without an open discussion (Climate Dynamics), it is, as the reviewer points out, not yet available. However, we anticipate that it should be accepted before we resubmit this manuscript. We will also add a short summary of the overturning circulation in the different scenarios to the results section.

7. I disagree with the potential usability of the quantification of the soft tissue pump on page 6, implying that the equations might be used as simplification in more complex models.

First. eq 6 should be deleted, since the change in atm CO2 can only be quantified once atm CO2 is calculated dynamically. Second, the ocenic DIC uptake (eq 5) has also as major weakness to deal with the overall setup, that include constant and identical CO2=270 ppm, which implies, that quantification have to be discussed with care. Here, they are taken as given quantification of the soft tissue pump, which might even be used elsewhere. I do not think, this is the case for the reason given above. Furthermore, the sentence, page 7, line 22 "In contrast, the model suggests that greater ocean ventilation rates in the glacial state would have led to reduced global DICsoft." and the following discussion is coming from nowhere and is not supported with any data. We know nothing on the ocean ventilation stage so far. Later-on, in section 4.7 it is argued, that interactive CO2 would only lead to minor effect. I strongly disagree, since the atmosphere-surface ocean gas exchange is a function of the pCO2 difference of both.

We include equation 6 in order to illustrate the approximately linear dependence of changes in CO_2 due to the soft tissue pump and the product of global export and ideal age of the ocean. As discussed above, the major differences in DIC(total) due to setting atmospheric CO_2 to 270 ppm should be in the DIC(sat) term. Our calculations are based on a prescribed atmospheric value of CO2 of 270 ppm; thus, using the equation $R = (\Delta CO_2/CO_2)/(\Delta DIC/DIC)$, we simply substitute equation 5 for $\Delta DIC(soft)$, the global average DIC(total) for DIC, CO_2 = 270 ppm and R = 10, we derive equation 6. But we do not mean to use this to ignore the intricacies of this or any other general circulation model; our aim is simply to demonstrate how these three variables appear to be related in these scenarios, in order to improve the conceptual understanding. Because it is common the think about carbon reservoir changes in terms of atmospheric CO_2, we feel it is valuable to leave equation 6 as it is, but we will add a discussion to this section to clarify that this is indeed a simplification. We would also point out that Ödalen et al. (2017) independently made an almost identical simplification.

8. Whenever a statement is made, which variable change how much, which is also find in a figure, please include a reference to this figure.

Thank you for this suggestion; we will add these references.

9. The meaning of the four separations of DIC (DICsat, DICdis, DICsoft, DICcarb) are explained in the abstract, but not again in the introduction. I believe, this should be repeated around line 10 (page 2), to make the main text independent from the abstract.

Thank you for this suggestion; we will add this to the introduction.

10. page 2, line 24: "DICsoft depends ... on the flushing rate of the deep ocean which clears out accumulated DICsoft". This is a bit sloppy and not correct: DICsoft depends on the ocean circulation as a whole, the surface to deep ocean transport also transports it to the deep ocean.

We agree and will alter this phrasing.

11. page 3, line 11: "preformed DIC" is not explained/defined her, onlxy later on page 4.

We will add an explanation of preformed DIC to the introduction along with the description of the DIC decomposition (comment #9).

12. page 3, line 25f: "Here, we use a fully-coupled general circulation model (GCM) to investigate the potential importance of DICdis in altering air-sea CO2 partitioning on long

timescales." This aim of the paper is not given as such in the abstract, but should be contained there.

We will add this to the abstract as suggested.

13. page 3, line 30: "prescribe a constant CO2": It is not only constant in individual experiments, it is also identical in all experiments as 270 ppm. This should be clarified here directly, because it implies, that the atm CO2 is only a driver of climate, but not of carbon cycle changes.

We will clarify this at this point in the text.

14. page 4, line 5: "static land and ice sheet". Please explain, or should this read "static land ice sheets"?

Thank you for catching this; the list should read "…a sea ice module, static land, *and static* ice sheets." This will be changed in the text.

15. page 4, line 10: The paper Galbraith and de Lavergne (submitted) is missing in the reference list, but need to be included there, at best with a link to an accessible version. If not, maybe introduce this information only, once the paper is accessible somewhere, eg in the next iteration of the paper.

We will include this information in the bibliography. As noted (cf. #6), we expect that that paper will be accepted for publication before this manuscript is resubmitted and in any case before publication.

16. page 4, experiments: As already given above, the different CO2 levels should be transfered into ΔT. Also give a brief reasoning for your choices of CO2 here, e.g. why is the reference CO2 270 ppm, and not 278 ppm, as usual, why 607 and 911 ppm?

The reference CO_2 of 270 ppm is used as a simplification for interglacial CO_2. The radiative forcing is proportional to ln([CO_2]); thus, 405, 607 and 911 ppm are chosen as linear increments above 180 and 270 ppm (the former approximately represents glacial CO_2). This rationale will be added to the text on page 4, section 2.2.

17. page 4, experiments: Orbital parameters: Eccentricity seemed to have not changed, but nevertheless, state its values, and for which climate state it is typical. Also state, typical values of obliquity and precession for today and LGM.

This is correct: eccentricity is constant in all of these simulations. This as well as the values for obliquity and precession for modern and LGM conditions will be added to page 4, section 2.2.

18. page 4, line 17: Iron fertilization: Did I get it right, that the glacial dust fields only change iron availability, but not the radiative forcing? Please clarify. Furthermore, the field in the cited paper (Nickelsen and Oschlies 2015) are taken from Mahowald et al 2006, which should be state here. Also be aware (and potentially discuss), that, at least to my knowledge, more recent LGM dust fields of the Mahowald groud differ to the dust field published in 2006 (especially in the high-latitudes), (e.g. Albani et al 2012 (Clim Dyn), Albani et al 2016 (GRL), which might have an impact on Southern Ocean iron fertilization.

This is correct: the radiative forcing is not adjusted based on the dust field. This will be clarified in the text. We will also add the Mahowald et al. (2006) reference to page 4, line 17 and note the disagreement with more modern reconstructions.

19. page 5, line 18: "standard deviation of only 4 µmol/kg". I do not see any error bars in Fig 1, and in DICcarb the values vary by 20 to 35 µmol/kg. Something is wrong here.

As stated in the text (page 5, line 18: "over the entire range of CO_2 values"), this standard deviation is not an error bar for individual simulations, which are simply run to equilibrium, but rather the standard deviation of the values of DIC(carb) among all simulations. This will be clarified in the text.

20. page 5, line 23: "under nutrient depletion experiment". Which one would that be? I only see Fe fertilization expleriments, which would be the opposite.

This refers to the experiments run by Ito and Follows (2013), as indicated in the text. We did not conduct nutrient depletion experiments but, as noted, rather the opposite, in order to investigate the same dependence. We will clarify the phrasing here.

21. page 5ff: I suggest to combine "3 Results" and "4 Discussions" into "3 Results and Discussions" since sec 3 so far is pretty short and sec 4 also includes results.

We plan to restructure these two sections in the revision; thank you for the input.

22. page 6, line 30: Define "ideal age".

The ideal age tracer is a conservative tracer that is set to 0 in the surface ocean and increases by 1 for each model year in the ocean interior. This definition will be added to the first discussion of this tracer in the main text (page 5, line 21).

23. page 6, line 31,32: "quantitative strength of the relationship is striking". It is, what I would expect. The interesing part for me would actually be, to see the individual contribution of the two variables combined in Figure 3, so please also plot "global export" and "age" and define both precisely (are they averaged, if yes, over which results?).

The correlation with DIC(soft) and each of these parameters individually is lower than the correlation of DIC(soft) and the product of global export and age, which is why only the latter is presented here. Indeed, global export and age are individually averaged spatially over the global ocean for each simulation, and then the product of these two averages is taken. This will be clarified in the text (page 6, lines 29-30). We will also add the two additional panels, as suggested.

24. page 7, eq 5,6: These regressions equations are of very limited use, since atm CO2 has been kept constant at 270 ppm, and the gas exchange is a linear function of the atmosphere-surface ocean CO2 difference.

As in comment #7, these equations are given simply to illustrate the apparent linear relationship between global export * ocean age and DIC(soft), which can roughly be translated into a change in atmospheric CO_2 related to the soft tissue pump. Therefore, although coefficients in these equations are only derived empirically, we would argue that they add to the text by showing the relationship depicted in figure 3 mathematically.

25. page 7, line 22: We know nothing on ocean ventilations rates yet.

As in comment #6, we will add a brief summary of the central results of the Galbraith and de Lavergne paper, which will include the results of ocean circulation and ventilation in the different simulations.

26. page 8, line 2: Here surface and deep ocean are split at 1 km depth, but in Fig 5 at 500 m depth, Please be consistent.

Thank you for catching this inconsistency, which reflects a change in the choice of boundary in earlier versions of the manuscript; we will change this to consistently use 1 km for the boundary between the surface and deep ocean.

27. page 8, Eq 7: Here, the Southern Ocean contributen is termed fAABW, while in Eq 10 it is termed fSO. Please be consistent.

We consciously draw a distinction between f_{SO} (the fraction of water originating from the surface south of 30^{o}S) and f_{AABW}, which is not explicitly traced in the model but would be the true fraction of AABW. Similarly, we use f_{NAtl} and f_{NADW} to refer to the modeled approximation and true fractions of NADW, respectively. We will clarify this in the text (page 8, lines 7-8).

28. page 8, line 15: "hot and cold climate state": Be more precise what this means in terms of scenarios. This sentence probably refers to Fig 4, but no reference to it was given.

"Hot" and "cold" climate states refer to the extreme radiative forcing scenarios (CO_2 at 911 and 180 ppm, respectively). We will clarify this in the text and add a reference to figure 4 on page 8, line 15.

29. page 8: I suggest to combine the to subsection 4.2 and 4.3 to one subsection.

We will restructure these sections.

30. page 8, line 26: "when deep convection is occuring" When does it occur and where, scenario?

Deep convection in the model is sporadic in the simulations. The simulations with deep convection are those shown in figure 4 b. In the Southern Ocean, this includes all simulations; in the North Atlantic, this is all simulations at CO_2 = 180, 220, and 911 ppm, 1 (of 4) at CO_2 = 270 and 405 ppm, and 3 (of 4) at CO_2 = 607 ppm. We will allude to this in the text (page 8, line 26).

31. page 8, line 27: "... ventilation rates are high at both the cold and hot extremes". Show plot.

We will include a plot showing this.

32. page 9, line 9: O2;dis is not defined (I believe). You might add why O2 equilibrates an order of magnitude faster than CO2 (no bottleneck of the carbonate chemistry during oceanic uptake).

We will define O_2(dis) on page 9, line 6 (equivalent to DIC(dis), it is equal to the departure from equilibrium of O_2 in the surface ocean with respect to the atmosphere and advected into the ocean as a conservative tracer). Additionally, we will briefly discuss why it is able to equilibrate approximately an order of magnitude faster than DIC, as stated on page 9, lines 6-7.

33. page 9, line 11: "O2;dis in the SO is as high as 100 µmol/kg". I believe this is wrong, should be "as low as -100 µmol/kg", and the reference to the figure is needed (Fig 9). O2;dis seems to be largely anticorrelated to DICdis, but this was never mentioned as such.

We will change this in the text to read "The magnitude of O_2(dis) in the SO is as high as 100 µmol/kg" and add the reference to figure 9. We will also mention the anticorrelation.

34. page 9, line 21: "reduced sensitivity of export" to what?

We have written "reduced sensitivity *to* export;" this refers to the relationship between DIC(soft) and global export (cf. page 9, line 20). We will clarify this in the text.

35. page 9, last line: I do not undertstand why the two effects of iron fertilization and remineralization rate should be linearly additive.

We agree that this is not obvious from first principles, but it appears to be the case in this model. This is evidenced by the fact that DIC(Fe fert)-DIC(no Fe fert) for each of the DIC components is approximately the same using both remineralization rates under pre-industrial conditions, as shown in the first two panels of figure 2. We will clarify this in the text (page 9, lines 30-32).

36. page 10ff: Change NO_3 in NO_3^-

We will make this change.

37. page 10, line 13: What happens to you framework, if N:C ratios are not constant, as for example in postulated by Geider et al. (1998)?
Geider, R. J.; MacIntyre, H. L. Kana, T. M. A dynamic regulatory model of phytoplanktonic acclimation to light, nutrients, and temperature, Limnology and Oceanography, 1998, 43, 679-694.

This would indeed the possibility of calculating DIC(soft) from NO_3^-; i.e. equation 8 would no longer hold. The RMSE of the DIC(dis)+DIC(soft) is 5.2 µmol/kg; to achieve this error through changes in the N:C ratio only, this ratio would have to vary by more than 6%, which Geider et al. (1998) suggest is possible. However we still feel that this is an improvement on using preformed PO_4^{3-}, given that P:C varies much more dramatically (Geider and La Roche, 2002; Galbraith and Martiny, 2015). We will add a short discussion of this point to the text at the end of this section (page 11, line 18).

38. page 10ff: Unified framework: Here it is argued that the NO3;pre can be split in the contributions from Southern Ocean (SO), North Atlantic (NAtl) and North Pacific (NPac), later-on the argument is made that the North Pacific can be neglected due to missing deep convection. The contributions to DICdis;deep early in the draft (sec 4.2) was only split between NAtl and SO, but not NPac. Please be consistent in both approaches.

We will state earlier on page 10 that the contribution from the North Pacific is negligible and remove it from equation 10.

39. page 11, Eq 14 and 15: I have the feeling the factors Vi=Vtotal which are included in Eq 14 are missing in Eq 15, but should still be included here.

These are absorbed into the individual terms of global NO_3^-, NO_3^-(den), DIC(dis), and NO_3^-(pre). For example, NO_3^-(global) = V(deep)/V(total) * NO_3^-(deep) + V(upper)/V(total) * NO_3^-(upper). Thus, the volume terms drop out of equation 15.

40. page 11, line 17: RMSE: How has this been found? Is this the mean difference to the 1:1 line in Fig 10?

Yes, this is calculated from the modeled values of the different components (global average in each simulation) compared to the parametrized values (calculated from equation 15). We will clarify this in the text (page 11, lines 16-18).

41. page 11, Section 4.7: I think this section might be called "General discussion". I do not think the naming of "DICdis nadir" is helpful here, pleasxe consider other wording.

We will revise and rename this section.

42. page 12, lines 7-13: This paragraph is highly speculative and with the given support not justified. We know nothing on AABW formation for different climate state and the fixed, constant atmospheric CO2 boundary condition hinders in my view that such bold hypothesis are made based on the made analysis.

Indeed, this paragraph is deliberately speculative. This is stated in the text ("We do not claim that this soft upper limit was significant, but simply propose the possibility as a hypothesis that can be tested"). As such, we find it a useful contribution to the paper, as it points to a testable hypothesis for future work.

43. page 13, line 13: "ratio of remineralized to UTILIZED O2"

Thank you; we will add "utilized" to the text (page 13, line 13).

44. page 13, line 18ff: Preformed alkalinity (alkpre) is defined as total alkalinity at the surface. However, alkpre is then calculated from T, S, NO3, PO4. Does this imply, total alkalinity is not followed as an independent tracer in the carbon cycle of the ocean in the model? If not, this need some explanation, since normally the full carbon cycle needs 2 variables to be fully prognostic, typically the conservative tracers DIC and ALK are taken for that (from which pH, CO2, CO3, HCO3 are then calculated. Please clarify, and explain.

Preformed alkalinity was not included in the simulations. Therefore, as described at this point in the text, performed alkalinity has been a posteriori reconstructed as a linear function of temperature, salinity, and nutrients, similar to the approach used by Bernardello et al. (2014). This will be clarified in the text (page 13, line 18).

45. page 14: Eq A6 is trivial, its another version of Eq A1.

We will remove equation A6 from the text.

46. Figures: Make plots larger to have larger font size, include sub-plot names (eg Fig 1a,bc), check if units are always given (missing in Fig 11). In all figures each caption needs to have the full explanation of what is seen here (and not referring to Fig 1 as done so far).

We will increase the font sizes, include subplot labels, and write the marker key (as in figure 1) in each of the plots using this scheme (figures 3, 4, 5, and 10).

47. Fig 1: Plot all 5 subfigures on top of each other, planing, that this will fill 1 column in the final layout text, change x axis to ΔT, consider plotting it as bar charts, clarify what you mean in the caption with changed seaonality (probably a change in pressession).

We will plot the five subplots vertically and change the x-axis to ΔT. As above (cf. #4), we prefer to retain this plot style to demonstrate the relationship between DIC and radiative

forcing in this model. Indeed, "seasonality" refers to precession, which we will clarify in the caption.

48. Fig 2: If results are averages from 4 runs (as said here) give mean and error from averaging.

Indeed, this assertion is correct. As the means are given (these are the values plotted), we will include the standard deviations of the respective four runs as error bars and clarify this in the caption.

49. Fig 3: X axis: "Global export times age". "Global export" here implies only export of organic C or also CaCO3 export?

This refers to export of organic C only; we will clarify this in the figure caption.

50. Fig 4: Why do you take DICdis at 100m water, and not the average over the mixed layer?

We show DIC(dis) at 100 m depth given that we are using annual mean concentrations, and there is a strong seasonal cycle of mixed layer depths at high latitudes. The depth of 100 m was chosen keeping in mind that polar deep-water formation regions tend to have strong haloclines, and 100m tends to be below the summer mixed layer but within the winter mixed layer, and is therefore relatively representative of the mixed layer concentrations when deep waters are forming.

51. Fig 6,8,9,11: Define scenarios "glacial" and "interglacial". Are these averages over several scenarios? Unit is missing in Fig 6.

These are single scenarios where the CO_2, obliquity, precession, and ice sheet configuration are 180 ppm, 22º, 90º, and LGM for the "glacial" scenario and 270 ppm, 24º, 90º, and pre-industrial for the "interglacial" scenario, respectively. We will clarify this in methods and in the figure captions and will add the units of DIC(dis) (µmol/kg) to the caption of figure 6.

52. Fig 7: I find this figure, highly confusing (not clear what lines represent), and not necessary at all.

We agree and will remove this figure.

53. Fig 10: Caption: Please reduce text and refer to where the Eq is found in text, e.g. lower plot y axis follows Eq 15. I am not sure for the other 2 plots there is a complete Eq contained in the theoretical framework, if not, please extend.

We will cite equations 11, 12, and 15 in the caption and reduce the caption length by referring to the appropriate section of the text for details (section 4.6). As we note in the text, we only expand the equations for the deep ocean (page 11, lines 1-2), but the full equations for DIC(dis) and DIC(soft) follow analogously to equation 13.

54. Fig 11: I am not sure, this Fig is necessary.

We find this important to show where the parametrization used for preformed alkalinity induces errors in the DIC(dis) analysis (cf. #44), as this is the main source of uncertainty. Thus, we would prefer to retain this figure in the appendix.

References

Archer, D. E., Eshel, G., Winguth, A., Broecker, W., Pierrehumbert, R., Tobis, M., and Jacob, R.: Atmospheric pCO_2 sensitivity to the biological pump in the ocean, Global Biogeochemical Cycles, 14, 1219-1230, 10.1029/1999GB001216, 2000.

Bernardello, R., Marinov, I., Palter, J. B., Sarmiento, J. L., Galbraith, E. D., and Slater, R. D.: Response of the Ocean Natural Carbon Storage to Projected Twenty-First-Century Climate Change, Journal of Climate, 27, 2033-2053, 10.1175/jcli-d-13-00343.1, 2014.

Galbraith, E. D., and Martiny, A. C.: A simple nutrient-dependence mechanism for predicting the stoichiometry of marine ecosystems, Proceedings of the National Academy of Sciences, 112, 8199-8204, 10.1073/pnas.1423917112, 2015.

Geider, R., and La Roche, J.: Redfield revisited: variability of C:N:P in marine microalgae and its biochemical basis, European Journal of Phycology, 37, 1-17, 10.1017/S0967026201003456, 2002.

Geider, R. J., Maclntyre, H. L., and Kana, T. M.: A dynamic regulatory model of phytoplanktonic acclimation to light, nutrients, and temperature, Limnology and Oceanography, 43, 679-694, 10.4319/lo.1998.43.4.0679, 1998.

Ito, T., and Follows, M. J.: Air-sea disequilibrium of carbon dioxide enhances the biological carbon sequestration in the Southern Ocean, Global Biogeochemical Cycles, 27, 1129-1138, 10.1002/2013GB004682, 2013.

Mahowald, N. M., Muhs, D. R., Levis, S., Rasch, P. J., Yoshioka, M., Zender, C. S., and Luo, C.: Change in atmospheric mineral aerosols in response to climate: Last glacial period, preindustrial, modern, and doubled carbon dioxide climates, Journal of Geophysical Research: Atmospheres, 111, 10.1029/2005JD006653, 2006.

Ödalen, M., Nycander, J., Oliver, K. I. C., Brodeau, L., and Ridgwell, A.: The influence of the ocean circulation state on ocean carbon storage and CO_2 drawdown potential in an Earth system model, Biogeosciences Discuss., 1-42, 10.5194/bg-2017-166, 2017.

Sigman, D. M., and Boyle, E. A.: Glacial/interglacial variations in atmospheric carbon dioxide, Nature, 407, 859-869, 10.1038/35038000, 2000.

The devil's in the disequilibrium: sensitivity of ocean carbon storage to climate state and iron fertilization in a general circulation model
Sarah Eggleston and Eric D. Galbraith
bg-2017-328

Response: Reviewer 2

This study deals with an interesting aspect of the global carbon cycle, relevant to un- derstanding past natural changes of atmospheric CO2 mixing ratio reconstructed from geological archives. As such it is relevant to the readership of Biogeosciences.

The decomposition of Dissolved Inorganic Carbon (DIC) into component parts based on a process-driven approach is an established procedure in the literature. This main advance here is a detailed look at a particular component of DIC (the 'disequilibrium' DIC) that has been overlooked in some previous studies.

Generally, the literature is well covered by the references. Although, I believe DeVries et al. "The sequestration efficiency of the biological pump", GRL (2012) is directly relevant to Figure 3 in this study, and should be considered when the findings linked to figure 3 are discussed.

We agree this is a relevant references and will add it in the revision.

The main findings are the de-coupling of the DIC_dis from the (previously) expected behaviour based on DIC_soft in some circumstances. This is shown in a number of idealised numerical model experiments. This finding is important and relevant to the literature.

We thank the reviewer for their support.

Specifically, equation (15), figure (10) and the insight gained from these for the ide- alised simulations are important and deserve to be published provided they are found to be robust.

With the manuscript in its present form, I have some reservations as to whether the findings are robustly supported by the work undertaken. I am unable to say for certain if this can be addressed by re-writing of the manuscript, or would require altered or additional numerical model runs. Below I detail my concerns on this issue.

1. Understanding the methods described in the text and their relation to the figures.
   As noted by Anonymous Reviewer 1, this study uses a fixed and constant atmospheric CO2 mixing ratio of 270 ppm in the numerical model experiments. While I see nothing intrinsically wrong with this approach, the manuscript as it is does not adequately describe the impacts of this choice on their results.
   For example, consider Figure 1 and accompanying text: On p5 lines 15-17, the manuscript states how a constant CO_2 for gas exchange of 270 ppm is used. Then, the manuscript states how the largest changes in DIC_sat is driven by the changes in ln(CO_2). Figure 1 does indeed plot DIC_sat against CO_2 with CO_2 shown to vary.
   I do not understand this figure or the text: precisely how is DIC_sat a function of ln(CO_2) if a constant CO_2 of 270 ppm is used for gas exchange. If a constant CO_2 of 270 ppm is used for gas exchange in the numerical simulations, then surely the CO_2

cannot be changing on the axes in figure 1. Also, DIC_sat should always be calculated relative to a CO_2 of 270 ppm, and so DIC_sat will not change with ln(CO2).
The issue recurs in Figure 2, the caption to which indicates that some experiments are run at 180 ppm CO_2 concentration.
This confusion is critical for assessment of the manuscript in its current form (e.g. also see major point 2, which derives from this).
Note that there are other studies in this topic that have dealt with similar issues well. For example, Marinov et al (2008) (cited by this manuscript) uses GCM simulations with a fixed temperature for air-sea gas exchange, but a varying dynamical temperature for ocean circulation. In that manuscript, the issue is well described and the findings are clear.
Is the issue here that one CO_2 is used for the radiative forcing of climate, but another CO_2 is used for air-sea gas exchange?
I cannot tell precisely with the manuscript in its present form. If this is the case, then all mentions of CO_2 in ppm [and ln(CO2)] that are different from 270ppm could be converted to radiative forcing (in W/mˆ2) with respect to CO_2 = 270 ppm. For example, CO_2 = 180ppm would be re-defined as 'Glacial radiative forcing' (or a numerical radiative forcing of _ -2.2 W/mˆ2).
For example: P11 Line 20 to line 24 reads: "The model simulations show a clear minimum DIC_dis at intermediate CO_2 (270-405 ppm). : : : the CO_2 driving gas exchange : : : is held fixed at 270 ppm."
This could be changed to something like: "The model simulations show a clear minimum DIC_dis at intermediate Radiative Forcing (0 – 2.2 Wm-2). : : : the CO_2 driving gas exchange : : : is held fixed at 270 ppm."
I am currently confused by the way this issue is written about in the study. Please clarify.

Indeed, different CO_2 levels are used for the radiative forcing, which is varied from 180 to 911 ppm in these simulations, and CO_2 used for the biogeochemistry, including air-sea gas exchange, which is always 270 ppm. Given the similar confusion raised by Reviewer 1, we will refer only to the different climate forcings in terms of the mean surface temperature (ΔT). We feel this will alleviate a great deal of misunderstanding.

2. DIC_sat and DIC_dis definitions:
There are two ways of defining DIC_sat and DIC_dis in the present-day system of rising CO_2, or over different periods when CO_2 has changed in the past.
Firstly, you can define both DIC_sat and DIC_dis relative to some fixed atmospheric CO_2 concentration (such as the preindustrial). Or secondly, you can define them relative to the current atmospheric CO_2 concentration at a particular point in time (for example it would be relative to 180 ppm at the LGM, or _400ppm in the present day).
This choice makes a big difference. Consider the present day: if DIC_sat is defined relative to present day atmospheric CO_2 then DIC_dis is small in the surface ocean and negative in the deep ocean. However, if DIC_sat is defined relative to preindustrial CO_2 then DIC_dis is positive in the surface ocean and _ zero at depth.
In the original discussions of DIC_sat (p2, lines 14-17) and DIC_dis (p3, lines 14-34), it is unclear whether a fixed or rising CO_2 concentration will be used to define DIC_dis and DIC_sat.
It eventually becomes clear (I think) that in this study, the DIC_sat is calculated relative to a fixed CO_2 of 270 ppm (page 4, line 15). However, the point is only made when discussing the numerical model set up.

A clearer indication of how DIC_sat and DIC_dis are treated in this study from the outset is required. Especially given the confusing 'fixed but changing' CO_2 issue from my other major concern. If the experiments are run with CO_2=180ppm, and DIC_sat is defined relative to 270ppm then this will have a large impact on the results.

We agree this is potentially confusing. We will add text to the introduction to precisely define the terms, as we use them. We will also add a new figure to illustrate these important concepts clearly. In our usage, both DIC(sat) and DIC(dis) are determined only in the surface layer and are propagated into the interior by mixing and advection. Thus, under a transient change of CO_2, the surface values would evolve as the CO_2 changes, and the values propagated into the interior would follow.

The devil's in the disequilibrium: ~~sensitivity~~ multi-component analysis of ~~ocean~~ dissolved carbon ~~storage to climate state~~ and ~~iron fertilization~~ oxygen changes under a broad range of forcings in a general circulation model

Sarah Eggleston[1,*] and Eric D. Galbraith[1,2,3]

[1]Institut de Ciència i Tecnologia Ambientals (ICTA), Universitat Autònoma de Barcelona, 08193 Barcelona, Spain
[2]Institució Catalana de Recerca i Estudis Avançats (ICREA), Pg. Lluís Companys 23, 08010 Barcelona, Spain
[3]Department of Earth and Planetary Science, McGill University, Montreal, Quebec H3A 2A7, Canada
[*]Now at: Laboratory for Air Pollution & Environmental Technology, Empa, Überlandstrasse 129, 8600 Dübendorf, Switzerland

Correspondence to: S. Eggleston (sarah.eggleston@gmail.com)

Abstract. ~~Ocean dissolved inorganic carbon (DIC) storage can be conceptualized~~ The complexity of dissolved gas cycling in the ocean presents a challenge for mechanistic understanding and can hinder model intercomparison. One helpful approach is the conceptualization of dissolved gases as the sum of multiple, strictly-defined components. Here we decompose dissolved inorganic carbon (DIC) into four components: saturation (DIC_{sat}), disequilibrium (DIC_{dis}), carbonate (DIC_{carb}) and soft tissue (DIC_{soft}). ~~Among these, DIC_{dis} and DIC_{soft} have the potential for large changes that are relatively difficult to predict. Here we~~ The cycling of dissolved oxygen is simpler, but can still be aided by considering O_2, $O_{2_{sat}}$ and $O_{2_{dis}}$. We explore changes in ~~DIC_{soft} and DIC_{dis} in~~ these components within a large suite of simulations with a complex coupled climate-biogeochemical model, driven by changes in ~~orbital forcing~~astronomical parameters, ice sheets and ~~the radiative effect of CO_2. Both DIC_{dis} and DIC_{soft}~~ radiative forcing, in order to explore the potential importance of the different components to ocean carbon storage on long timescales. We find that both DIC_{soft} and DIC_{dis} vary over a range of 40 μmol/kg in response to the climate forcing, equivalent to changes in atmospheric pCO_2 on the order of 50 ppm for each. ~~We find~~ The most extreme values occur at the coldest and intermediate climate states. We also find significant changes in O_2 disequilibrium, with large increases under cold climate states. We find that, despite the broad range of climate states represented, changes in global DIC_{soft} can be ~~well-approximated~~ quantitatively approximated by the product of deep ocean ideal age and the global export production flux~~, while~~. In contrast, global DIC_{dis} is dominantly controlled by the fraction of the ocean filled by Antarctic Bottom Water (AABW). Because the AABW fraction and ideal age are inversely correlated ~~between~~ among the simulations, DIC_{dis} and DIC_{soft} are also inversely correlated, dampening the overall changes in DIC. This inverse correlation could be decoupled if changes in deep ocean mixing were to alter ideal age independently of AABW fraction, or if independent ecosystem changes were to alter export and remineralization, thereby modifying DIC_{soft}. As an example of the latter, we show that iron fertilization causes both DIC_{soft} ~~to increase, and causes~~ and DIC_{dis} to ~~also increase by a similar or greater amount, to a degree that depends on~~ increase and that the relationship between these two components depends on the climate state. We propose a simple framework to consider the

global contribution of $DIC_{soft} + DIC_{dis}$ to ocean carbon storage as a function of the surface preformed nitrate and DIC_{dis} of dense water formation regions, the global volume fractions ventilated by these regions, and the global nitrate inventory. More extensive sea ice increases DIC_{dis}, and when sea ice becomes very extensive it also causes significant O_2 disequilibrium, which may have contributed to reconstructions of low O_2 in the Southern Ocean during the glacial. Global DIC_{dis} reaches a minimum near modern CO_2 because the AABW fraction reaches a minimum, which may have contributed to preventing further CO_2 rise during interglacial periods.

1 Introduction

The controls on ocean carbon storage are not yet fully understood. Although potentially very important, given the large inventory of dissolved inorganic carbon (DIC) the ocean contains (currently 38,000 Pg C vs. 700 Pg C in the pre-industrial atmosphere), the nuances of carbon chemistry, the dependence of air-sea exchange on wind stress and sea ice cover, the intricacies of ocean circulation, and the activity of the marine ecosystem all contribute to making it a very complex problem. The scale of the challenge is such that, despite decades of work, the scientific community has not yet been able to satisfactorily quantify the role of the ocean in the natural variations of pCO_2 between 180 and 280 ppm that occurred over ice age cycles. This failure reflects persistent uncertainty that also impacts our ability to accurately forecast future ocean carbon uptake . (Le Quéré et al., 2007; Friedlingstein et al., 2014).

In order to help with process understanding, DIC can be theoretically divided among four components that , together, determine the Volk and Hoffert (1985) proposed conceptualizing ocean carbon storage as consisting of a baseline surface-ocean average, enhanced by two "pumps" that transfer carbon to depth: the solubility pump, produced by the vertical temperature gradient, and the soft-tissue pump, produced by the sinking and downward transport of organic matter. This conceptualization proved very useful, but it fails to deal explicitly with the role of spatially- and temporally-variable air-sea partitioning of the "active" carbon inventory: exchange, and cannot effectively address changes in ocean circulation. A number of other conceptual systems have been employed (e.g. Broecker et al., 1985; Gruber et al., 1996), both for considering natural changes in the carbon cycle of the past and the anthropogenic transient input of carbon into the ocean.

Here, we use the decomposition laid out by Williams and Follows (2011), with the small change that we consider only DIC, rather than total carbon. This theoretical framework defines four components that, together, add up to the total DIC: saturation (DIC_{sat},), disequilibrium (DIC_{dis}, DIC_{soft} and DIC), carbonate (DIC_{carb} (Ito and Follows, 2013; Bernardello et al., 2014)) and soft tissue (DIC_{soft}) (Ito and Follows, 2013; Bernardello et al., 2014; Ödalen et al., 2018). The first two components are "preformed" quantities ($DIC_{pre} = DIC_{sat} + DIC_{dis}$), i.e. they are defined in the surface layer of the ocean and are carried passively by ocean circulation in the interior, while into the interior. In contrast, the latter two are equal to zero in the surface layer and accumulate in the interior due to biogeochemical activity . (see fig. 1). Note that the four components are diagnostic quantities

only, intended to aid in understanding mechanisms and clarifying hypotheses, and do not influence the behavior of the model (although they can be calculated more conveniently by including additional ocean model tracers, as described in Methods).

Saturation DIC ~~(DIC_{sat})~~ is simply determined by the atmospheric CO_2 concentration and its solubility in seawater, which is a function of ocean temperature, salinity, and alkalinity. For example, cooling the ocean will increase CO_2 solubility, thereby leading to an increase in DIC_{sat}. Given known changes in temperature, salinity, alkalinity, and atmospheric pCO_2, the effective storage of DIC_{sat} can be calculated precisely.

~~The soft tissue pump (see e.g. Toggweiler et al., 2003) has been defined in various ways, but universally involves the uptake of DIC in the surface ocean by marine primary producers~~ At the ocean surface, primary producers take up DIC. The organic carbon that is formed then sinks or is subducted (as dissolved or suspended organic matter) and is transformed into remineralized DIC within the water column (a small fraction is buried at depth). Here we define DIC_{soft} as that ~~accumulated by~~ which accumulates through the net respiration of organic matter below the top layer of the ocean (in our model, the uppermost 10 m). Thus, DIC_{soft} depends both on the export flux of organic matter, affected by surface ocean conditions including ~~iron supply (Martin, 1990), and on the~~ nutrient supply (Moore et al., 2013; Martin, 1990), and the ocean circulation as a whole, including the surface-to-deep export and the flushing rate of the deep ocean, which clears out accumulated DIC_{soft} (Toggweiler et al., 2003). The Southern Ocean (SO) is thought to be an important region for such changes on glacial/interglacial timescales, as the ecosystem there is currently iron-limited, and it also plays a major role in deep ocean ventilation ~~(Martin, 1990; Toggweiler et al., 2003; Jac furthermore, the degree of stratification may have changed significantly on these timescales (François et al., 1997; Sigman et al., 2010)~~(Mar Assuming a constant global oceanic phosphate inventory and constant C:P ratio, DIC_{soft} would be stoichiometrically related to the preformed PO_4 ~~(PO_{4pre})~~ (PO_{4pre}^{3-}) inventory of the ocean, where PO_{4pre}^{3-} is the concentration of PO_4^{3-} in newly-subducted waters, and a ~~passive~~ passively-transported tracer in the interior. The potential to use PO_{4pre}^{3-} as a metric of DIC_{soft} prompted ~~significant~~ very fruitful efforts to understand how it could change over time (Ito and Follows, 2005; Marinov et al., 2008a; Goodwin et al., 2008), though it has been pointed out that the large variation in C:P of organic matter ~~weakens~~ could weaken the relationship between DIC_{soft} and PO_{4pre} ~~(Galbraith and Martiny, 2015). Dissolved O_2 can potentially serve as a better metric of DIC_{soft}, given the relatively small variations in the O_2:C of respiration compared to the relatively high variability in C:P (Martiny et al., 2013). But Apparent Oxygen Utilization (AOU), typically taken as a measure of accumulated respiration, can be misleading if the preformed O_2 concentration differed significantly from saturation (Ito et al., 2004; Duteil et al., 2013). Thus, despite being conceptually simple, DIC_{soft} can be difficult to quantify observationally.~~ $^{3-}_{4pre}$ (Galbraith and Martiny, 2015). Given that the variability of N:C is significantly smaller than P:C (Martiny et al., 2013), we use preformed nitrate in the discussion below.

Similar to DIC_{soft}, DIC_{carb} is defined here as the DIC generated by the dissolution of calcium carbonate shells below the ocean surface layer. Note that this does not include the impact that shell production has at the surface; calcification causes alkalinity to decrease in the surface ocean, raising surface ~~pp~~pCO_2 and shifting carbon to the atmosphere. Rather, within the framework used here, this effect on alkalinity distribution falls under DIC_{sat}, since it alters the solubility of DIC. This highlights an important distinction between the four-component framework, which strictly defines subcomponents of DIC, and the "pump"

frameworks, which provide looser descriptions of vertical fluxes of carbon and, in some cases, alkalinity. Changes in DIC_{carb} on the timescales of interest are generally thought to be small compared to those of DIC_{sat} and DIC_{soft}.

Typically, only these three components are considered as the conceptual drivers behind changes in the air-sea partitioning of ~~p~~pCO_2 (e.g., IPCC, 2007; Kohfeld and Ridgwell, 2009; Marinov et al., 2008a; Goodwin et al., 2008). However, a fourth component, ~~disequilibrium carbon (~~DIC_{dis}~~)~~, is also potentially significant as discussed by Ito and Follows (2013). Defined as the difference between preformed DIC and DIC_{sat}, DIC_{dis} can be relatively large (Takahashi et al., 2009) because of the slow timescale of atmosphere-surface ocean equilibrium of carbon compared to other gases, caused by the ~~buffering capacity of seawater (e.g., Zeebe and Wolf-Gladrow, 2001; Broecker and Peng, 1974).~~ reaction of CO_2 with seawater (e.g., Zeebe and Wolf-Gladrow, 2001; Broecker and Peng, 1974; Galbraith and Martiny, 2015). In short, DIC_{dis} is a function of all non-equilibrium processes on DIC in the surface ocean, including biological uptake, ocean circulation, and air-sea fluxes of heat, freshwater and CO_2.

Like DIC_{sat}, DIC_{dis} is a conservative tracer determined in the surface ocean, with no sources or sinks in the ocean interior. Since the majority of the ocean is filled by water originating from small regions of the Southern Ocean and the North Atlantic, the net whole-ocean disequilibrium carbon is approximately determined by the DIC_{dis} in these areas weighted by the fraction of the ocean volume filled from each of these sites. Unlike the other three components, DIC_{dis} could contribute either additional oceanic carbon storage ($DIC_{dis} > 0$) or reduced oceanic carbon storage ($DIC_{dis} < 0$). ~~Studies~~ Although this parameter is implicitly included in most models, studies using preformed nutrients as a metric for biological carbon storage have often ignored the potential importance of DIC_{dis} by assuming fast air-sea gas exchange (e.g., Marinov et al., 2008a; Ito and Follows, 2005). In the pre-industrial ocean this is of little importance, given that global DIC_{dis} is small because the opposing effects of North Atlantic and Antarctic water masses largely cancel each other. However, Ito and Follows (2013) showed that DIC_{dis} can have a large impact by amplifying changes in DIC_{soft} under constant pre-industrial ocean circulation, and ~~the possibility~~ Ödalen et al. (2018) have very recently shown that DIC_{dis} ~~varied~~ can vary significantly in response to changes in ocean circulation states~~has not been thoroughly explored.~~.

The cycling of dissolved oxygen is simpler than DIC. Because O_2 does not react with seawater or the dissolved constituents thereof, it has no dependence on alkalinity, and its equilibration with the atmosphere through air-sea exchange occurs approximately one order of magnitude faster than DIC (on the order of one month, rather than one year). Nonetheless, dissolved oxygen can be conceptualized as including a preformed component, which is the sum of saturation and disequilibrium, and an oxygen utilization component, which is given by the difference between the in situ and preformed O_2 in the ocean interior. Apparent Oxygen Utilization (AOU), typically taken as a measure of accumulated respiration, can be misleading if the preformed O_2 concentration differed significantly from saturation, i.e. if $O_{2_{dis}}$ is significant, as it appears to be in high latitude regions of dense water formation (Ito et al., 2004; Duteil et al., 2013; Russell and Dickson, 2003). If $O_{2_{dis}}$ varies with climate state, it might contribute significantly to past or future oxygen concentrations.

Here, we use a ~~fully-coupled general circulation model (GCM)~~ complex Earth system model to investigate the potential ~~importance of DIC~~ $_{dis}$ ~~in altering air-sea CO~~changes in the constituents of DIC and O_2 ~~partitioning~~ on long timescales, relevant for past climate states as well as the future. We make use of a large number of equilibrium simulations, conducted over a

wide range of ~~CO_2~~radiative, orbital and ice sheet boundary conditions, as a "library" of contrasting ocean circulations in order to test the response of disequilibrium carbon storage to physically plausible changes in ocean circulation. The basic physical aspects of these simulations were described by Galbraith and de Lavergne (2018). We supplement these with a smaller number of iron fertilization experiments to examine the additional impact of circulation-independent ecosystem changes. In order to simplify the interpretation, we chose to prescribe a constant pCO_2 of 270 ppm for the air-sea exchange in all simulations, as also done by Ödalen et al. (2018). Thus, the changes in DIC_{sat} reflect only changes in temperature, salinity, alkalinity and ocean circulation arising from the climate response, and not changes in pCO_2. Nor do they explicitly consider changes in the total carbon or alkalinity inventories driven by changes in outgassing and/or burial (Roth et al., 2014; Tschumi et al., 2011); rather, the alkalinity inventory is fixed, and the carbon inventory varies due to changes in total ocean DIC (since the atmosphere is fixed). As such, the experiments here should be seen as idealized climate-driven changes, and should be further tested with more comprehensive models including interactive CO_2.

2 Methods

2.1 Model description

The GCM used in this study is CM2Mc, the Geophysical Fluid Dynamics Laboratory's Climate Model version 2 but at lower resolution (3°), described in more detail by Galbraith et al. (2011) and modified as described by Galbraith and de Lavergne (2018). This includes the Modular Ocean Model version 5, a sea ice module, static land~~and~~, and static ice sheets, and a module of Biogeochemistry with Light, Iron, Nutrients and Gases (~~BLINGv2~~BLINGv1.5) (Galbraith et al., 2010). Unlike BLINGv0, ~~BLINGv2~~ BLINGv1.5 allows for variable ~~stoichiometry~~ P:C stoichiometry using the "Line of Frugality" (Galbraith et al., 2015) and calculates the mass balance of phytoplankton in order to prevent unrealistic bloom magnitudes at high latitudes, reducing the magnitude of disequilibrium O_2, which was very high in BLINGv0 (Duteil et al., 2013; Tagliabue et al., 2016). In addition, three water mass tracer tags are defined: a Southern tracer south of 30°S, a North Atlantic tracer north of 30°N in the Atlantic, and a North Pacific tracer north of 30°N in the Pacific. An "ideal age" tracer is also defined as zero in the global surface layer, and increasing in all other layers at a rate of 1 year per year.

2.2 Experimental design

~~The basic setup of all model runs is identical to Galbraith and de Lavergne (submitted)~~ The model runs analyzed here are part of the same suite of simulations discussed by Galbraith and de Lavergne (2018). A control run was conducted with ~~atmospheric CO_2 set~~ a radiative forcing equivalent to 270 ppm atmospheric pCO_2 and the Earth's obliquity and precession set to modern values (23.4° and 102.9°, respectively). Experimental simulations were run at values of obliquity (22°, 24.5°) and precession (90°, 270°) representing the astronomical extremes encountered over the last 5 My (Laskar et al., 2004)~~. Solar radiation was varied at~~ , while eccentricity was held constant at 0.03. A range of greenhouse radiative forcings was imposed equivalent to pCO_2 levels ~~equivalent to~~ of 180, 220, 270, 405, 607, ~~and~~ or 911 ppm~~. The biologeochemical~~ ; with reference

to a pre-industrial radiative forcing, the radiative forcings are roughly equal to -2.2, -1.1, 0, $+2.2$, $+4.3$, and $+6.5$ W/m^2, respectively (Myhre et al., 1998).

The biogeochemical component of the model calculates air-sea carbon fluxes using a fixed atmospheric pCO$_2$ of 270 ppm throughout all model runs~~, irrespective of the~~. Note that 270 ppm was chosen to reflect an average interglacial level, rather than specifically focusing on the pre-industrial climate state. This use of constant pCO$_2$ for the carbon cycle means that the DIC$_{sat}$ is not consistent with the pCO$_2$ used for ~~radiative forcing.~~ the radiative forcing, so that changes in DIC$_{sat}$ caused by a given pCO$_2$ change would tend to be larger than would be expected in reality. This has a negligible effect on the other carbon components, given that they do not depend directly on pCO$_2$; this has been confirmed by model runs with the University of Victoria Earth System Model using a similar decomposition strategy (Khatiwala et al., *in prep.*).

Eight additional runs were conducted using Last Glacial Maximum (LGM) ice sheets with ~~CO$_2$ of 180 and 220 ppm and~~ the lowest two radiative forcings and the same orbital parameters. Iron fertilization simulations ~~use the~~ calculate the input flux of dissolved iron to the ocean surface assuming a constant solubility and using the glacial atmospheric dust field of Mahowald et al. (2006) as modified by Nickelsen and Oschlies (2015) instead of the standard pre-industrial dust field; note that this is not entirely in agreement with more modern reconstructions, which could potentially have an influence on the induced biological blooms, both in magnitude and geographically (e.g. Albani et al., 2012, 2016). Four iron fertilization experiments were run ~~at an atmospheric CO$_2$ of 180 ppm with~~ with the lowest radiative forcing with LGM ice sheets, as well as one model run similar to the control run. Finally, two simulations were run that were identical to the pre-industrial setup, but the rate of remineralization of sinking organic matter is set to 75% of the default rate, approximately equivalent to the expected change due to a 5^{o}C ocean cooling (Matsumoto et al., 2007); one of these runs also includes iron fertilization. All simulations are summarized in Table 1.

~~The~~ In the following, three particular runs are highlighted for comparison to illustrate cold (CW), moderate (MW), and hot (HW) worlds. These include radiative forcings of -2.2, 0, and $+4.3$ W/m^2, respectively; the former includes LGM ice sheets; and the obliquity and precession is 22^o and 90^o for GL and 22^o and 270^o for PI and WP. These specific runs are distinguished from glacial-like (GL) and interglacial-like (IG) scenarios, which refer to averages of four runs each, each with a radiative forcing of -2.2 and 0 W/m^2, respectively; the GL runs also have LGM ice sheets.

All simulations were run for 2100 – 6000 model years beginning with a pre-industrial spinup. While the model years presented here largely reflect runs after having reached steady state, it is important to note that the pre-industrial run (41 in Table 1) still has a drift of 1 μmol/kg over the 100 y shown here and thus may not yet be at steady state.

2.3 ~~DIC decomposition~~Decompositions

~~Following Ito and Follows (2013) and Bernardello et al. (2014), we separate the total DICinto preformed and remineralized DIC(DIC~~The four-component DIC scheme and three-component O$_2$ scheme described in the introduction can be exactly calculated for any point in an ocean model using five easily-implemented ocean model prognostic tracers: DIC, DIC$_{pre}$ ~~and~~

~~DIC_{rem}).~~

$DIC = DIC_{pre} + DIC_{rem}$

~~DIC~~, DIC_{sat}, O_2 and O_{2pre}, since: $DIC_{dis} = DIC_{pre} - DIC_{sat}$, $DIC_{soft} = (O_{2pre} - O_2) \cdot r_{C:O_2}$, $DIC_{dis} = DIC - DIC_{pre} - DIC_{soft}$, and $O_{2dis} = O_{2pre} - O_{2sat}$ (O_{2sat} can be accurately calculated from the conservative tracers temperature and salinity). In the absence of a DIC_{sat} tracer, it can be estimated from alk_{pre} ~~is set equal to DIC at the surface and is propagated into the ocean interior as a conservative tracer. It in turn is the sum of two components: the first is the DIC at equilibrium with the atmosphere (DIC~~, temperature and salinity. For this large suite of simulations, we only had DIC, alk, O_2 and O_{2pre} available. Thus, although we could calculate O_{2dis} and DIC_{soft} directly, it was necessary to use an indirect method to calculate the other three carbon tracers. Following Bernardello et al. (2014), we first estimate alk_{pre} using a regression, then calculate DIC_{sat} using alk_{pre}, temperature, salinity, and the known atmospheric pCO_2 of 270 ppm. DIC_{carb} is calculated as $0.5 \cdot (alk - alk_{pre})$, and DIC_{dis} is then calculated as a residual. For more details and an estimate of the error in the method, see the appendix.

3 Results and Discussion

3.1 General climate response to forcings

Differences in the general ocean state among the model simulations are described in detail by Galbraith and de Lavergne (2018). We provide here a few key points, important for interpreting the dissolved gas simulations. First, the AABW fraction of the global ocean varies over a wide range among the simulations, with abundant AABW under low and high global average Surface Air Temperature (SAT), and a minimum at intermediate SAT (fig. 2(b)). The NADW fraction is approximately the inverse of this. The ventilation rate of the global ocean is roughly correlated with the AABW fraction, with rapid ventilation (small average ideal age) when the AABW fraction is high (fig. 2). The density difference between AABW and NADW is the overall driver of the AABW fraction and ventilation rate in the model simulations. The density difference can be explained, in all simulations colder than present-day, by the effect of sea ice cycling in the Southern Ocean on the global distribution of salt: when the Southern Ocean is cold and sea ice formation abundant, there is a large net transport of freshwater out of the circum-Antarctic, causing AABW to become more dense. NADW becomes consequently fresher, because there is less salt left to contribute to NADW. As noted by Galbraith and de Lavergne (2018), the ~~second is the disequilibrium term, defined as the degree of under- or oversaturation (DIC_{dis}).~~

$DIC_{pre} = DIC_{sat} + DIC_{dis}$

simulated ventilation rates should be viewed with caution, given the poor mechanistic representation of diapycnal mixing in the deep ocean, and the AABW fraction may not be correlated with ventilation rate in the real ocean.

~~Within the mixed layer, plankton take up DIC to produce organic matter or calcium carbonate shells, both of which sink or are subducted and are remineralized in the water column to inorganic carbon (DIC_{soft} and DIC_{carb}, respectively).~~

$DIC_{rem} = DIC_{soft} + DIC_{carb}$

~~DIC_{sat}, DIC_{soft}, and DIC_{carb} can be calculated explicitly from the model tracers (for more details, see the appendix), and DIC_{dis} is then calculated as a residual.~~

$$DIC_{dis} = DIC - DIC_{sat} - DIC_{soft} - DIC_{carb}$$

4 ~~Results~~

3.1 ~~Climate experiments~~General changes in DIC

Total DIC generally decreases from cold to warm simulations, under the constant pCO_2 of 270 ppm used for air-sea exchange. Changes in DIC_{sat} drive the largest portion of this trend, decreasing approximately linearly with ~~ln(CO_2)~~ surface air temperature due to the temperature-dependence of CO_2 solubility, resulting in a difference of 50 μmol/kg over this range (see fig. 3). ~~DIC~~Because of the constant pCO_2 of 270 ppmv in the biogeochemical module, the simulated range of DIC_{sat} is larger than would occur if the prescribed biogeochemical pCO_2 were the same as that used to produce the low SAT (Ödalen et al., 2018). DIC_{carb} is relatively small in magnitude ~~with~~ and generally increases with SAT, but has a standard deviation of only 4 μmol/kg over ~~the entire range of CO_2 values, and~~ all simulations, so we do not discuss it further.

In contrast to DIC_{sat} and DIC_{carb}, DIC_{dis} and DIC_{soft} vary nonlinearly with global temperatures, with a clear and shared turning point ~~at a radiative forcing near a CO_2 concentration of about 400 ppm.~~ near the middle of the temperature range. Thus, the extreme values of DIC_{soft} and DIC_{dis} occur under the coldest state and at an intermediate state close to the pre-industrial. Both DIC_{dis} and DIC_{soft} are strongly correlated with ocean ventilation, quantified here by the global average of the ideal age tracer (r^2 = 0.69 and 0.89, respectively), and thus with each other (r^2 = 0.74). However, ~~in contrast to the findings of Ito and Follows (2013) , who~~ whereas Ito and Follows (2013) found a positive correlation of DIC_{soft} and DIC_{dis} under nutrient depletion experiments with constant climate, these experiments indicate that, when driven by the wide range of physical changes explored here, DIC_{soft} ~~and DIC_{dis} are negatively correlated under the range of climate states under constant iron supply explored here.~~

3.2 ~~Iron fertilization experiments~~

~~The impact of increasing the dust flux to the ocean on DIC_{soft} depends strongly on the ocean circulation state (see fig. A). In the pre-industrial climate state (middle panel), half of the total oceanic C inventory change (14.6 μmol/kg) is due to increased soft tissue pump storage ($\Delta$and DIC_{soft} = 7.3 μmol/kg). This is qualitatively the same in the case that the remineralization rate of organic carbon is reduced by 25% (left panel). However, in the high-ventilation runs under glacial-like conditions (right panel), the change in total DIC is somewhat reduced (11.1 μmol/kg) and ΔDIC_{soft} is small (SO average 4.3 μmol/kg; global average 2.9 μmol/kg). DIC_{dis} is also dependent on the ocean circulation, but in the opposite direction: the change is more significant (9.4 μmol/kg global average) in the glacial-like simulations compared to the pre-industrial simulation (6.4 μmol/kg). Each of these values rises when considering only the SO (13.4 and 9.0 μmol/kg, respectively). In both the pre-industrial and glacial-like simulations, changes in DIC_{dis} constitute an important part of the total change. DIC_{carb} is reduced to a small extent~~

by iron fertilization, due to the reduced nutrient content of AAIW/SAMW and consequent decrease in low latitude carbonate production, which raises low latitude surface ocean alkalinity, causing an increase in DIC_{sat}. are negatively correlated.

4 Discussion

Simulated changes in DIC_{dis} are of the same magnitude as the DIC_{soft} changes, to which much greater attention has been paid. For a global average buffer factor between 8 and 14 (Zeebe and Wolf-Gladrow, 2001), a rough, back-of-the-envelope calculation shows that a 1 μmol/kg change in DIC corresponds to a 0.9 – 1.5 1.6 ppm change in atmospheric $pp\mathrm{CO}_2$ based on a DIC concentration of 2300 μmol/kg and $p\mathrm{CO}_2$ of 270 ppm. Thus, the increase in the global average DIC_{dis} in these simulations of 16 μmol/kg (pre-industrial control) to 62 μmol/kg (LGM-like conditions with Fe fertilization) could have accounted for could have contributed more than a 40 – 70 ppm difference in atmospheric ppm change in the atmospheric $p\mathrm{CO}_2$ stored in the ocean during the glacial compared to today. While the It is important to recognize that the drawdown of CO_2 by disequilibrium storage would have resulted in a decrease of DIC_{sat}, given the dependence of the saturation concentration on $p\mathrm{CO}_2$, so this estimate should not be interpreted as a straightforward atmospheric $p\mathrm{CO}_2$ change. Nonetheless, while this is only a first-order approximation and the model biases are potentially large, it seems very likely that the desquilibrium disequilibrium carbon storage was a significant portion of the net 90 ppm difference.

Below, we discuss the changes in DIC_{soft} and DIC_{dis} that result from the CO_2, orbital and ice-sheet driven climate changes. We then discuss related changes in disequilibrium O_2, implications for preformed nutrient theory, and propose a new mechanism that may have helped to prevent the Earth from warming its way out of the ice age cycle.

3.1 Climate-driven changes in DIC_{soft}

The biogeochemical model used here is relatively complex, with limitation by three nutrients (N, P and Fe), denitrification and N_2 fixation, in addition to the temperature- and light-dependence typical of biogeochemical models. The climate model is also complex, including a full atmospheric model, a highly-resolved dynamic ocean mixed layer, and many nonlinear subgridscale parameterizations, and uses short (< 3 h) timesteps. The simulations we show span a wide range of behaviours, including major changes in ocean ventilation pathways and patterns of organic matter export.

Thus, it is perhaps surprising that the net global result of the biological pump, as quantified by DIC_{soft}, has highly predictable behavior. As shown in fig. 4, the global DIC_{soft} varies closely with the product of the global average sinking flux of organic matter at 100 m and the average ideal age of the global ocean. Qualitatively this is not a surprise, given that greater export pumps more organic matter to depth, and a large age provides more time for respired carbon to accumulate within the ocean. But the quantitative strength of the relationship is striking. As demonstrated in fig. 4, global DIC_{soft} is not as well correlated with either of these parameters separately as it is with their produce, "age × export."

It is difficult to assess the likelihood that the real ocean follows this relationship to a similar degree. One reason it might differ is if remineralization rates vary spatially, or with climate state. In the model here, as in most biogeochemical models, organic matter is respired according to a globally-uniform power law relationship vs. depth (Martin et al., 1987). Kwon et al.

(2009) showed that ocean carbon storage is sensitive to changes in these remineralization rates, and this would provide an additional degree of freedom. It is not currently known how much remineralization rates can vary naturally; they may vary as a function of temperature (Matsumoto et al., 2007) or ecosystem structure. As a result, the relationship between DIC_{soft} and ~~ideal ocean age multiplied by global~~ age × export may be stronger in the model than in the real ocean.

Nonetheless, the results suggest that, as a useful first-order approximation, the global change in DIC_{soft} between two states can be given by ~~:~~ a simple linear regression:

$$\Delta DIC_{soft}[\mu mol\ kg^{-1}] = 0.036 m_1 \cdot \Delta(export[Pg\ C\ y^{-1}] \cdot age[y] \times export[Pg\ C\ y^{-1}]) \quad (1)$$

or in terms of pCO_2 ~~terms and assuming a buffer factor of 10~~:

$$\Delta CO_2[ppm] \approx m \cdot \Delta(export[Pg\ C\ y^{-1}] \cdot age[y])$$

~~where $m = 0.065, 0.042, 0.029$ for modern~~

$$\Delta pCO_{2,soft}[ppm] \approx m_2 \cdot \Delta(age[y] \times export[Pg\ C\ y^{-1}]) \quad (2)$$

Note that m_2 is a function of the buffer factor and the climate state (atmospheric pCO_2 and DIC). Based on the results here, $m_1 = 0.036$ and $m_2 = 0.065, 0.042, 0.029$ for modern (405 ppm pCO_2), pre-industrial ~~and glacial conditions respectively.~~ (270 ppm) and glacial (180 ppm) conditions, respectively. Note that we have not varied pCO_2 in these simulations, so these equations are only meant to illustrate the mathematical relationship observed in fig. 4. This simple meta-model may provide a useful substitute for full ocean-ecosystem calculations, and ~~could~~ should be further tested against other ocean-ecosystem coupled models ~~.~~ with interactive CO_2. Note that, as for the disequilibrium estimate above, the soft tissue pump CO_2 drawdown would be partially compensated by a decrease in saturation carbon storage, so this will be larger than the net atmospheric effect. In addition, we have not accounted for consequent changes in the surface ocean carbonate chemistry (including changes in the buffer factor).

It is important to point out that the simulated change in DIC_{soft} between interglacial and glacial states ~~is~~ appears to be in conflict with reconstructions of the LGM. Proxy records appear to show that LGM dissolved oxygen concentrations were lower throughout the global ocean, with the exception of the North Pacific, implying greater DIC_{soft} concentrations during the glacial then during the Holocene ~~(Galbraith and Martiny, 2015)~~(Galbraith and Jaccard, 2015). In contrast, the model suggests that greater ocean ventilation rates in the glacial state (fig. 2(a)) would have led to reduced global DIC_{soft}. As discussed by ~~Galbraith and de Lavergne (submitted)~~Galbraith and de Lavergne (2018), radiocarbon observations imply that the model ideal age is approximately 200 y too young under glacial conditions ~~,~~ compared to the LGM, suggesting a circulation bias that may reflect incorrect diapycnal mixing or non-steady-state conditions. Whatever the cause, if we take this 200 y bias into account, the regression implies an additional 33 $\mu mol\ kg^{-1}$ DIC_{soft} were stored in the glacial ocean. This would bring the simulated glacial DIC_{soft} close to, but still less than, the simulated pre-industrial value.

We propose that the apparent remaining shortfall in simulated glacial DIC_{soft} could reflect one or more of the following non-exclusive possibilities: 1. the model does not capture changes in remineralization rates caused by ecosystem changes; 2. the

model underestimates the glacial increase in the nitrate inventory and/or growth rates, perhaps due to changes in the iron cycle; 3. the ocean was not in steady state during the LGM, and therefore not directly comparable to the ~~"glacial"~~ GL simulation; 4. the inference of DIC_{soft} from proxy oxygen records is incorrect due to significant changes in preformed oxygen disequilibrium (see below). If either of the first two possibilities is important, it would imply an inaccuracy in the meta-model derived here.

3.2 Climate-driven changes in DIC_{dis}~~: volume fractions~~

The ocean basins below 1 km depth are largely filled by surface waters subducted to depth in regions of deepwater formation (Gebbie and Huybers, 2011). In our simulations, water originating in the surface North Atlantic, termed NADW, and the Southern Ocean, termed AABW, make up 80-96% of this total deep ocean volume. Thus, to first order, the deep average DIC_{dis} concentration can be approximated by a simple mass balance:

$$DIC_{dis_{deep}} \approx f_{AABW} \cdot DIC_{dis_{AABW}} + f_{NADW}(1 - f_{AABW}) \cdot DIC_{dis_{NADW}} \quad (3)$$

Here, f_{AABW} ~~and f_{NADW} represent~~ represents the fraction of deepwater originating in the SO~~and North Atlantic and $DIC_{dis_{AABW,NADW}}$~~, and $DIC_{dis_{AABW}}$, $DIC_{dis_{NADW}}$ represent the DIC_{dis} ~~concentration~~ concentrations at the sites of deepwater formation (see fig. 5). North Atlantic deep waters form with negative DIC_{dis}, reflecting surface undersaturation, while the Southern Ocean is supersaturated ($DIC_{dis} > 0$)~~, and these~~. These opposing tendencies between NADW and AABW cause a partial cancellation of DIC_{dis} when globally averaged~~.~~, which makes the disequilibrium component small in the modern ocean. Theoretically, the simulated DIC_{dis} could change either due to changes in f_{AABW} or the end-member compositions. Although the exact values of DIC_{dis} in the two polar oceans vary ~~over time~~ among the simulations in response to climate (the reasons for which are discussed in more detail below), these changes are small relative to the consistent large contrast between ~~AABW and NADW~~ f_{AABW} and f_{NADW}, so that deep DIC_{dis} is strongly controlled by the global balance of AABW vs. NADW in each simulation (see fig. 6). Global DIC_{dis} becomes much larger when f_{AABW} is larger, similar to the dynamic evoked by Skinner (2009). This is also illustrated by the depth transects of DIC_{dis} in fig. A.

~~In this model, both the cold and the hot climate states~~ We estimated the concentration of DIC_{dis} in the regions of AABW and NADW formation, shown in fig. 5(b). The end members vary less significantly than f_{AABW} over the range of simulations, in part due to competing effects of different processes. As discussed in section 3.1, simulations at both the low and high radiative forcing values used show increased AABW production, with a minimum at intermediate values ~~. The AABW/NADW fractions are determined by the relative density of surface waters in the two polar ocean basins, as discussed in more detail by Galbraith and de Lavergne (submitted). The~~ (fig. 5). The fact that the highest $DIC_{dis_{AABW}}$ occurs at low SAT can be attributed to the rapid formation rate of AABW, while the intermediate-SAT minimum in AABW ~~is thus responsible for~~ volume explains the minimum in global ocean DIC_{dis} (fig. 3). ~~In addition,~~ We note that expanded terrestrial ice sheets shift the ratio of AABW to NADW to higher values, due to their impact on NADW temperature and downstream expansion of Southern Ocean sea ice ~~(Galbraith and de Lavergne)~~(Galbraith and de Lavergne, 2018), further increasing DIC_{dis} in glacial-like conditions.

3.3 ~~Climate-driven changes in DIC_{dis}: end members~~

~~Due to the general dominance of AABW in the deep ocean, the concentration of DIC_{dis} in the regions of AABW formation, $DIC_{dis_{AABW}}$, is another important factor determining global DIC_{dis}. This varies less significantly than f_{AABW} over the range of simulations, in part due to competing effects of different processes. Surface ocean DIC_{dis} in the Southern Ocean grows in response to upwelling of deepwater, which brings DIC-charged waters to the surface, thus contributing to the carbon super-saturation. Thus, when deep convection is occurring, the rapid injection of carbon to the surface tends to inflate DIC_{dis}. Like the f_{AABW}, ventilation rates (as quantified by global ideal age) are high at both the cold and hot extremes (Galbraith and de Lavergne, submitted), also contributing to the intervening minimum in DIC_{dis} in the AABW formation regions.~~

Sea ice in the Southern Ocean ~~exerts~~ would be expected to exert a further control over DIC_{dis}, as this reduces air-sea gas exchange, thus allowing carbon to accumulate beneath the ice. ~~The total sea ice cover decreases continuously from the low to high CO_2 simulations (fig. **??**), but DIC_{dis} is markedly higher in the glacial-like scenarios compared to $CO_2 = 270$ or 911 ppm (fig. **??** and A). In the glacial state, high~~ However we did not perform experiments to isolate this effect.

3.3 Climate-driven changes in $O_{2_{dis}}$

Similarly to DIC_{dis} ~~is a widespread characteristic of the sea surface, whereas in the 270 and 911 ppm simulations, high DIC_{dis} only occurs in regions of AABW formation during episodes of deep convection. Terrestrial ice sheets cause an increase in the magnitude of DIC_{dis} both in the Southern Ocean and the North Atlantic. Due to the opposing signs in the two regions, these effects partially compensate each other, but the volumetric dominance of AABW causes its DIC_{dis} increase to win out, raising global DIC_{dis}.~~

3.4 ~~Disequilibrium O_2~~

~~$O_{2_{dis}}$ is also sensitive to sea ice cover, but with a pronounced difference from DIC_{dis}. Because~~ , $O_{2_{dis}}$ is defined as the departure from equilibrium of O_2 in the surface ocean with respect to the atmosphere and is advected into the ocean as a conservative tracer. Unlike C, O_2 does not react with seawater, and is present only as dissolved diatomic oxygen. Thus, O_2 has a much shorter time scale of exchange at the ocean-atmosphere interface, equilibrating one order of magnitude faster than CO_2. As a result, it is not sensitive to sea ice as long as there remains a fair degree of open water (Stephens and Keeling, 2000). But as the sea ice concentration approaches complete coverage, O_2 equilibration rapidly becomes quite sensitive to sea ice. If there is a significant undersaturation of O_2 in upwelling waters, the disequilibrium can become quite large (fig. 8).

In the model simulations, the ~~magnitude of~~ $O_{2_{dis}}$ in the Southern Ocean ~~is as high as 100 μ~~becomes as large as -100μmol/kg in the coldest states (note that DIC_{dis} and $O_{2_{dis}}$ are often anti-correlated). Because the disequilibrium depends on the O_2 depletion of waters upwelling at the Southern Ocean surface, ~~it~~ this could potentially be even ~~higher~~larger, if upwelling waters had lower O_2. ~~This suggests the~~ We do not place a large degree of confidence in these values, given the likely sensitivity to poorly-resolved details of sea ice dynamics (e.g. ridging, leads) and dense water formation. Nonetheless, the potential for very large disequilibrium oxygen under cold states prompts the hypothesis that very extensive sea ice cover over most of the exposure pathway in the Southern Ocean might have made a significant contribution to the low O_2 concentrations reconstructed for the glacial (Jaccard et al., 2016; Lu et al., 2015).

3.4 Iron ~~fertilization-driven changes in DIC_{soft} and DIC_{dis}~~ fertilization experiments

In addition to the changes driven by ice sheets, orbital and radiative forcing, we conducted iron fertilization experiments under glacial and pre-industrial-like conditions, including a simulation with reduced remineralization rates (fig. A). As expected, both the global export and DIC_{soft} increase when ~~dust~~ iron deposition is increased. However, the DIC_{soft} increase is significantly lower in the well-ventilated ~~glacial-like~~ GL simulations (2.9 μmol/kg) compared to the ~~interglacial-like~~ PI simulation (7.3 μmol/kg). This difference is qualitatively in accordance with the age ~~multiplied by~~ $\times$ export relationship (fig. 4), though with a smaller increase of DIC_{soft} than would be expected from the export increase, compared to the broad spectrum of climate-driven changes. This reduced sensitivity ~~to~~ of DIC_{soft} to the global export can be attributed to the fact that the iron-enhanced export occurs in the Southern Ocean, ~~where~~ presumably because the remineralized carbon can be quickly returned to the surface by upwelling when ventilation is strong. Thus, the impact of iron fertilization on DIC_{soft} is strongly dependent on Southern Ocean circulation.

The iron addition also causes an increase of DIC_{dis} ~~,~~ of approximately equal magnitude to DIC_{soft} in the ~~interglacial-like simulation ,~~ PI simulation and of relatively greater proportion in the ~~glacial-like~~ GL simulations. Because the ocean in the ~~glacial-like~~ GL simulations is strongly ventilated, ~~with extensive sea ice cover in the Southern Ocean, the~~ the increase in export leads to an increase of DIC_{dis}, as remineralized DIC_{soft} is ~~rapidly~~ returned to the Southern Ocean surface, where it has a relatively short residence time ~~and the extensive sea ice inhibits~~ that limits outgassing to the atmosphere. ~~Thus, with~~ With rapid Southern Ocean circulation~~and extensive sea ice cover~~, a good deal of the DIC sequestered by iron fertilization ends up in the form of DIC_{dis}, rather than DIC_{soft} as ~~frequently assumed. Furthermore, experiments~~ might be assumed. Thus, just as the glacial state has a larger general proportion of DIC_{dis} compared to DIC_{soft}, the iron addition under the glacial state produces a larger fraction of DIC_{dis} relative to DIC_{soft}. The experiment in which the remineralization rate was reduced by 25% ~~indicate~~ indicates that the effects of iron fertilization alone on both DIC_{soft} and DIC_{dis} are quite insensitive to the remineralization rate (see fig. ~~A) Thus, the~~ A); for total DIC as well as for each component, the difference between the iron fertilization run and the corresponding control run in similar in panels (a) and (b). While we have not run a simulation under glacial-like conditions with a reduced remineralization rate, this suggests that the effects of iron fertilization and changes in the remineralization rate can be well-approximated as being linearly additive in this model.

The tendency to sequester carbon as DIC_{dis} vs. DIC_{soft}, in response to iron addition, can be quantified by the global ratio $\Delta DIC_{dis}/\Delta DIC_{soft}$. Our experiments suggest that this ratio is 0.9 for the pre-industrial state and 3.3 for the glacial-like state. Because of the circulation dependence of this ratio, it is expected that there could be significant variation between models. It is worth noting that Parekh et al. (2006) found $\Delta DIC_{dis}/\Delta DIC_{soft}$ of 2 in response to iron fertilization, using a modern ocean circulation, as analyzed by Ito and Follows (2013). We also ~~caution~~ note that the quantitative values of DIC_{soft} and DIC_{dis} resulting from the altered iron flux should be taken with a grain of salt, given the very large uncertainty in ~~models of iron cycling~~ iron cycling models (Tagliabue et al., 2016).

These results provide a note of caution for interpreting iron fertilization model experiments, which might be assumed to act primarily on the soft tissue carbon storage. At moderate ventilation rates (the pre-industrial control run), an increase in iron

results in an increase both in DIC_{soft}, due to higher biological export, and DIC_{dis}, because of the upwelling of C-rich water resulting from higher remineralization, the effect discussed by Ito and Follows (2013). However, under a high ventilation state there is only a small increase in DIC_{soft} in response to increased Fe in the surface ocean, as the remineralized carbon is quickly returned to the surface, thus producing a significant increase in DIC_{dis} only. Thus, the carbon storage resulting from Southern Ocean iron addition could actually be dominated by DIC_{dis} under some climate states, so that the overall impact may be significantly larger than would be predicted from DIC_{soft} and/or O_2 utilization.

3.5 A unified framework for DIC_{dis} and preformed nutrients

The concept of preformed nutrients allowed the production of a very useful body of work, striving for simple predictive principles. This work highlighted the importance of the nutrient concentrations in polar oceans where deep waters form (Sigman and Boyle, 2000; Ito and Follows, 2005; Marinov et al., 2008a) as well as changes in the ventilation fractions of AABW and NADW, given their very different preformed nutrient concentrations (Schmittner and Galbraith, 2008; Marinov et al., 2008b). Although the variability of P:C ratios implies significant uncertainty for the utility of $PO_{4_{pre}}^{3-}$ in the ocean, the relative constancy of N:C ratios suggests that $NO_{3_{pre}}^{-}$ is indeed linked to DIC_{soft}, inasmuch as the global N inventory is fixed (Galbraith and Martiny, 2015).

However, as shown by the analyses here, DIC_{soft} – reflected by the preformed nutrients – is only half the story. Changes in DIC_{dis} can be of equivalent magnitude, and can vary independently of DIC_{soft} as a result of changes in ocean circulation and sea ice. Nonetheless, we find that the same conceptual approach developed for DIC_{soft} can be used to predict DIC_{dis} from the end member DIC_{dis} and the global volume fractions. The preformed relationships and DIC_{dis} can therefore be unified as follows (see fig. 10):

$$DIC_{soft} = NO_{3_{rem}}^{-} \cdot r_{C:N} \tag{4}$$

Remineralized nitrate can be expressed in terms of the global nitrate inventory and the accumulated nitrate loss due to pelagic and benthic denitrification~~, analagous to AOU:~~ :

$$NO_{3_{rem}}^{-} = NO_{3_{global}}^{-} - NO_{3_{pre}}^{-} + NO_{3_{den}}^{-} \tag{5}$$

$$NO_{3_{pre}}^{-}{}_{3_{pre_{upper}}} \approx f_{SO}{}_{SO,upper} \cdot NO_{3_{pre_{SO}}}^{-}{}_{3_{pre_{SO,upper}}} + f_{NAtl}{}_{NAtl,upper} \cdot NO_{3_{pre_{NAtl}}}^{-}{}_{3_{pre_{NAtl,upper}}} + f_{NPac}{}_{NPac,upper} \cdot NO_{3_{pre_{NPac}}}^{-}{}_{3_{pre_{NPac,upper}}} \tag{6}$$

$$NO_{3_{pre_{deep}}}^{-} \approx f_{AABW} \cdot NO_{3_{pre_{AABW}}}^{-} + f_{NADW} \cdot NO_{3_{pre_{NADW}}}^{-} \tag{7}$$

~~Above, for simplicity, we consider only the deep ocean DIC_{dis}. Now, however, we would like to include the upper ocean (above 1 km) as well.~~ Because there is production of intermediate water but no deep convection in the North Pacific, we calculate this mass balance for the upper ocean (above 1 km) and deep ocean separately, dropping the ~~final term in Eq.?? in the calculation below 1 km:~~

$$DIC_{soft_{deep}} \approx r_{C:N} \cdot [NO_{3_{deep}} + NO_{3_{den,deep}} - (f_{SO,deep} \cdot NO_{3_{pre_{SO,deep}}} + f_{NAtl,deep} \cdot NO_{3_{pre_{NAtl,deep}}})]$$

~~The same calculations, including the North Pacific component, are performed to obtain $DIC_{soft_{upper}} + DIC_{dis_{upper}}$; here we expand only the deep ocean component for simplicity.~~ Pacific Ocean term in eq. 7 for the deep ocean. For brevity, we continue with the derivation for the deep ocean only; the upper ocean follows analogously.

$$DIC_{soft_{deep}} \approx r_{C:N} \cdot [NO_{3_{deep}}^{-} + NO_{3_{den,deep}}^{-} - (f_{AABW} \cdot NO_{3_{pre_{AABW}}}^{-} + f_{NADW} \cdot NO_{3_{pre_{NADW}}}^{-})] \tag{8}$$

Combining with equation 3,

$$\begin{aligned} DIC_{dis_{deep}} + DIC_{soft_{deep}} \approx & r_{C:N} \cdot (NO_{3_{deep}}^{-} + NO_{3_{den,deep}}^{-}) + f_{SO,deepAABW} \cdot (DIC_{dis_{SO,deep}dis_{AABW}} - r_{C:N} \cdot NO_{3_{pre_{SO,deep}}3_{pre_{AABW}}}^{-}) \\ & + f_{NAtl,deepNADW} \cdot (DIC_{dis_{NAtl,deep}dis_{NADW}} - r_{C:N} \cdot NO_{3_{pre_{NAtl,deep}}3_{pre_{NADW}}}^{-}) \end{aligned} \tag{9}$$

Finally, the global average is computed by summing the volume-weighted values in the upper and deep ocean:

$$DIC_{dis_{global}} + DIC_{soft_{global}} \approx [V_{upper} \cdot (DIC_{dis_{upper}} + DIC_{soft_{upper}}) + V_{deep} \cdot (DIC_{dis_{deep}} + DIC_{soft_{deep}})]/V_{total} \tag{10}$$

Fully expanded, this yields:

$$\begin{aligned} DIC_{dis_{global}} + DIC_{soft_{global}} \approx & \frac{V_{upper}}{V_{total}} [r_{C:N} \cdot (NO_{3_{upper}}^{-} + NO_{3_{den,upper}}^{-}) + f_{SO,upper} \cdot (DIC_{dis_{SO,upper}} - r_{C:N} \cdot NO_{3_{pre_{SO,upper}}}^{-}) \\ & + f_{NAtl,upper} \cdot (DIC_{dis_{NAtl,upper}} - r_{C:N} \cdot NO_{3_{pre_{NAtl,upper}}}^{-})] \\ & + \frac{V_{deep}}{V_{total}} [r_{C:N} \cdot (NO_{3_{deep}}^{-} + NO_{3_{den,deep}}^{-}) + f_{SO,deepAABW} \cdot (DIC_{dis_{SO,deep}dis_{AABW}} - r_{C:N} \cdot NO_{3_{pre_{SO,deep}}3_{pre_{AABW}}}^{-}) \\ & + f_{NAtl,deepNADW} \cdot (DIC_{dis_{NAtl,deep}dis_{NADW}} - r_{C:N} \cdot NO_{3_{pre_{NAtl,deep}}3_{pre_{NADW}}}^{-})] \end{aligned} \tag{11}$$

which can be generalized for any number n of ventilation regions i as:

$$DIC_{dis_{global}} + DIC_{soft_{global}} \approx r_{C:N} \cdot (NO_{3_{global}}^{-} + NO_{3_{den,global}}^{-}) + \sum_{i=1}^{n} f_i \cdot (DIC_{dis_i} - r_{C:N} \cdot NO_{3_{pre_i}}^{-}) \tag{12}$$

Thus, total carbon storage as soft and disequilibrium carbon (i.e. everything other than DIC_{sat} and DIC_{carb}) varies with the global nitrate inventory, corrected for ~~NO_3^-~~ accumulated NO_3^- loss to denitrification, and the difference between DIC_{dis} and ~~$r_{C:N} \cdot NO_{3_{pre}}$~~ $r_{C:N} \cdot NO_{3_{pre}}^{-}$ in the polar oceans, modulated by their respective volume fractions. ~~It is interesting that this relationship is more accurate than either DIC_{dis} or DIC_{soft}, among our suite of simulations, with an RMSE of 3.6, 7.0 and 5.2 μmol kg^{-1} for $DIC_{dis} + DIC_{soft}$, DIC_{dis} and DIC_{soft}, respectively.~~

3.6 ~~DIC_{dis} nadir and peak CO_2~~

~~The model simulations show a clear minimum of DIC_{dis} at intermediate CO_2 (270 – 405 ppm). This occurs as a result of the minimum contribution of AABW to the global ocean, and to a lesser extent, a minimum in the DIC_{dis} of AABW. A minimum global extent of AABW during interglacials has been documented from ϵ_{Nd} (Piotrowski et al., 2005), and it has been shown that~~

~~AABW likely ceased to form entirely for a brief portion of the last interglacial, marine isotope stage 5e (Hayes et al., 2014). Although the model has biases that prevent a strict interpretation of the CO_2 and orbital combination at which this nadir is likely to occur, its robust emergence from the relative density control on deep water ventilation volumes makes its existence appear reasonable (Galbraith and de Lavergne, submitted).~~

~~We suggest that the nadir of DIC_{dis} may have contributed to a "soft" upper limit on CO_2 during interglacials. Galbraith and Eggleston (20~~ ~~that the lower limit of CO_2 over glacial cycles is quite firm and that low CO_2 is very common. In addition, they showed that, although the peak values of CO_2 during interglacials vary significantly, interglacial CO_2 levels are relatively common, suggesting that they are also a preferred state. We propose that the DIC_{dis} nadir would have contributed to preventing a significant CO_2 rise above interglacial CO_2, since a rise of temperatures above that which gives the DIC_{dis} nadir will increase AABW formation and thereby draw down CO_2 as DIC_{dis}. Of course this would be counteracted by an increase of DIC_{soft}, if it were to behave opposite of DIC_{dis}, as occurs in our simulations – whether or not this is true depends on unresolved climate dependencies in the marine ecosystem, which currently remains an open question. We do not claim that this soft upper limit was significant, but simply propose the possibility as a hypothesis that can be tested~~Although this nitrogen-based framework avoids the problem of C:P variability, it is not clear how large the effects of variable C:N might be in the real world. This could be a worthy topic for future exploration.

4 Conclusions

~~Carbon storage in the ocean can be quantified~~ The conceptualization of ocean carbon storage as the sum of the saturation, soft tissue, carbonate, and disequilibrium components can greatly assist in enhancing mechanistic understanding (Williams and Follows, 2011; I Our simulations indicate that the ~~latter~~ disequilibrium component may play a very important role, which has ~~been largely neglected in other studies~~not been broadly appreciated. Changes in the ~~climate state~~ physical climate states, as simulated by our model, tend to drive the soft tissue ~~pump~~ and the disequilibrium ~~pump~~ components in opposite directions. However, this is not necessarily true in the real ocean, given that the simulated ~~anticorrelation~~ anti-correlation is not mechanistically required, but instead arises from the fact that f_{AABW} and ~~ideal age · export are anticorrelated~~ age × export are anti-correlated in the simulations. On the contrary, the radiocarbon analysis of Galbraith and de Lavergne (2018) suggests that the glacial ocean age was significantly greater than in the corresponding simulations, implying that this anti-correlation does not hold in reality. Our iron fertilization experiments explore another aspect of this decoupling, in which age × export increases despite no change in f_{AABW}. There is plenty of scope for these to have varied in additional ways in the real world, not captured by our ~~idealized simulations.~~ simulations, including the idealized mechanisms explored by Ödalen et al. (2018). Although the anti-correlation of DIC_{dis} and DIC_{soft} in our simulations results in small overall changes, their magnitudes are sufficient that their total scope for change exceeds that required to explain the glacial/interglacial CO_2 change.

~~Iron fertilization experiments are a popular method of testing the sensitivity of pCO~~Our results also show a surprising capacity for O_2 ~~to an increase in dust flux to the Southern Ocean; here, these simulations illustrate the non-linearity of the effects of circulation and increased primary productivity on DIC. At moderate ventilation rates (the pre-industrial control run),~~

~~an increase in iron results in an increase both in DIC_{soft}, due to higher biological export, and DIC_{dis}, because of the upwelling of C-rich water resulting from higher remineralization. However, under a "glacial" state, high ventilation in this model produces only a small increase in DIC_{soft} in response to increased Fe in the surface ocean, as the remineralized carbon is quickly returned to the surface, thus producing a significant increase in DIC_{dis} only. This also raises an important warning for iron fertilization studies: the CO~~disequilibrium to develop in a cold state. We suggest that this reflects a high sensitivity of O_2 to sea ice when sea ice coverage reaches very high fractions. This generally unrecognized potential for sea ice coverage to cause large oxygen undersaturation may have contributed to very low O_2 ~~impact of Southern Ocean iron addition can actually be dominated by the DIC_{dis}, so that the overall impact may be significantly larger than would be predicted from DIC_{soft} and~~in the Southern Ocean during glacial periods, as suggested by foraminiferal I/~~or O_2 utilization~~Ca measurements (Lu et al., 2015).

The results presented here suggest that disequilibrium carbon should be considered as a major component of ocean carbon storage, linked to ocean circulation ~~, sea ice~~ and biological export in non-linear and ~~interdepenent~~ interdependent ways. Despite these nonlinearities, ~~we~~ the simulations suggest that the resulting global carbon storage can be well-approximated by ~~a simple relationship~~ simple relationships. We propose one such relationship, including the global nitrate inventory, and the DIC_{dis} and preformed ~~CO_3~~ NO_3^- in ocean ventilation regions (eq. 12). ~~The glacial simulations suggest that disequilibrium carbon may have been the dominant component of oceanic carbon uptake during cold phases of the ice age cycles.~~ As this study represents the result of a single model, prone to bias, it would be very useful to test our results using other GCMs including additional biogeochemical complexity. It would also be useful to consider how disequilibrium carbon can change under future ~~pp~~CO_2 levels, including developing observational constraints on its past and present magnitude, and exploring the degree to which inter-model variations in DIC_{dis} may contribute to uncertainty in climate projections.

Code availability. All model runscripts, code and simulation output are freely available from the authors, or can be obtained by download from https://earthsystemdynamics.org/cm2mc-simulation-library.

Appendix A: DIC decomposition

DIC is treated as the sum of four components:

$$DIC = DIC_{sat} + DIC_{dis} + DIC_{soft} + DIC_{carb} \quad \text{(A1)}$$

DIC_{sat} is the DIC at equilibrium with the atmosphere given the surface ocean temperature, salinity, and alkalinity and the atmospheric ~~pp~~CO_2 calculated following Zeebe and Wolf-Gladrow (2001):

$$DIC_{sat} = f(T, S, alk_{pre}, pCO_2) \quad \text{(A2)}$$

In this model, DIC_{soft} is proportional to the utilized O_2, which is defined as the difference between preformed and total O_2, where the ratio of remineralized C to utilized O_2 ($r_{C:O_2}$) is 106:150.

$$DIC_{soft} = r_{C:O_2} \cdot (O_{2_{pre}} - O_2) \quad \text{(A3)}$$

DIC derived from $CaCO_3$ dissolution is proportional to the change in alkalinity, correcting for the additional change in alkalinity due to hydrogen ion addition during organic matter remineralization.

$$\mathrm{DIC_{carb}} = 0.5 \cdot [(\mathrm{alk} - \mathrm{alk_{pre}}) + r_{\mathrm{N:O_2}} \cdot (\mathrm{O_{2_{pre}}} - \mathrm{O_2})] \tag{A4}$$

Preformed alkalinity, defined as the total alkalinity at the surface and treated as a conservative tracer, ~~was reconstructed here annually~~ is calculated within the model framework but was not written out during the model runs. Therefore, we have reconstructed this parameter a posteriori for each model year through multilinear regressions as a function of century-averaged salinity (S), temperature (T), and preformed O_2, NO_3^- and PO_4^{3-}~~.~~, following the approach of Bernardello et al. (2014).

$$\begin{aligned}\mathrm{alk_{pre}} =& (a_0 + a_1 \cdot \mathrm{S'} + a_2 \cdot \mathrm{T'} + a_3 \cdot \mathrm{O_{2_{pre}}} + a_4 \cdot \mathrm{NO^-_{3_{pre}}} + a_5 \cdot \mathrm{PO^{3-}_{4_{pre}}}) \cdot \mathrm{NAtl} \\ &+ (b_0 + b_1 \cdot \mathrm{S'} + b_2 \cdot \mathrm{T'} + b_3 \cdot \mathrm{O_{2_{pre}}} + b_4 \cdot \mathrm{NO^-_{3_{pre}}} + b_5 \cdot \mathrm{PO^{3-}_{4_{pre}}}) \cdot \mathrm{SO} \\ &+ (c_0 + c_1 \cdot \mathrm{S'} + c_2 \cdot \mathrm{T'} + c_3 \cdot \mathrm{O_{2_{pre}}} + c_4 \cdot \mathrm{NO^-_{3_{pre}}} + c_5 \cdot \mathrm{PO^{3-}_{4_{pre}}}) \cdot (1 - \mathrm{SO} - \mathrm{NAtl})\end{aligned} \tag{A5}$$

where $\mathrm{S'} = \mathrm{S} - 35$, $\mathrm{T'} = \mathrm{T} - 20^{\circ}\mathrm{C}$, the a_i are determined by a regression in the surface North Atlantic, the b_i for the SO, and the c_i using the model output elsewhere in the surface. The tracers SO and NAtl are set to 1 in the surface Southern Ocean (south of 30°S) and the North Atlantic (north of 30°N), respectively, and are conservatively mixed into the ocean interior. This parametrization induces an uncertainty on the order of 1 μmol/kg in globally averaged $\mathrm{DIC_{dis}}$ (see fig. A1). As discussed above, however, this is small compared to the signal seen over all simulations.

Finally, $\mathrm{DIC_{dis}}$ has been back-calculated from the model output as a residual.

$$\mathrm{DIC_{dis}} = \mathrm{DIC} - \mathrm{DIC_{sat}} - \mathrm{DIC_{soft}} - \mathrm{DIC_{carb}}$$

Author contributions. E. D. Galbraith conducted the model simulations, S. Eggleston performed the analysis, and both contributed to writing the manuscript.

Competing interests. The authors declare that they have no conflict of interest.

Acknowledgements. The authors would like to thank R. Bernardello for very helpful discussion. S. Eggleston ~~is~~ was funded by a fellowship from the Swiss National Science Foundation. E. D. Galbraith acknowledges computing support from the Canadian Foundation for Innovation and Compute Canada, and financial support from the Spanish Ministry of Economy and Competitiveness, through the María de Maeztu Programme for Centres/Units of Excellence in R&D (MDM-2015-0552).

References

Albani, S., Mahowald, N. M., Delmonte, B., Maggi, V., and Winckler, G.: Comparing modele and observed changes in mineral dust transport and deposition to Antarctica between the Last Glacial Maximum and current climates, Clim. Dyn., 38, 1731–1755, doi:10.1007/s00382-011-1139-5, 2012.

Albani, S., Mahowald, N. M., Murphy, L. N., Raiswell, R., Moore, J. K., Anderson, R. F., McGee, D., Bradtmiller, L. I., Delmonte, B., Hesse, P. P., and Mayewski, P. A.: Paleodust variability since the Last Glacial Maximum and implications for iron inputs to the ocean, Geophys. Res. Lett., 43, doi:10.1002/2016GL067911, 2016.

Bernardello, R., Marinov, I., Palter, J. B., Sarmiento, J. L., Galbraith, E. D., and Slater, R. D.: Response of the Ocean Natural Carbon Storage to Projected Twenty-First-Century Climate Change, J. Climate, 27, 2033–2053, doi:10.1175/jcli-d-13-00343.1, 2014.

Broecker, W. S. and Peng, T.-H.: Gas exchange rates between air and sea, Tellus, 26, 21–35, 1974.

Broecker, W. S., Takahashi, T., and Takahashi, T.: Sources and flow patterns of deep-ocean waters as deduced from potential temperature, salinity, and initial phosphate concentration, Journal of Geophysical Research, 90, 6925–6939, doi:10.1029/JC090iC04p06925, http://onlinelibrary.wiley.com/doi/10.1029/JC090iC04p06925/abstract, 1985.

Duteil, O., Koeve, W., Oschlies, A., Bianchi, D., Galbraith, E., Kriest, I., and Matear, R.: A novel estimate of ocean oxygen utilisation points to a reduced rate of respiration in the ocean interior, Biogeosciences, 10, 7723–7738, doi:10.5194/bg-10-7723-2013, 2013.

François, R., Altabet, M. A., Yu, E.-F., Sigman, D. M., Bacon, M. P., Frank, M., Bohrmann, G., Bareille, G., and Labeyrie, L. D.: Contribution of Southern Ocean surface-water stratification to low atmospheric CO_2 concentrations during the last glacial period, Nature, 389, 929–935, doi:10.1038/40073, 1997.

Friedlingstein, P., Meinshausen, M., Arora, V. K., Jones, C. D., Anav, A., Liddicoat, S. K., and Knutti, R.: Uncertainties in CMIP5 climate projections due to carbon cycle feedbacks, J. Climate, 27, 511–526, 2014.

Galbraith, E. and de Lavergne, C.: Response of a comprehensive climate model to a broad range of external forcings: relevance for deep ocean ventilation and the development of late Cenozoic ice ages, Clim. Dyn., doi:10.1007/s00382-018-4157-8, 2018.

Galbraith, E. D. and Eggleston, S.: A lower limit to atmospheric CO_2 concentrations over the past 800,000 years, Nat. Geosci., 10, 295–298, doi:10.1038/ngeo2914, 2017.

Galbraith, E. D. and Jaccard, S. L.: Deglacial weakening of the oceanic soft tissue pump: global constraints from sedimentary nitrogen isotopes and oxygenation proxies, Quaternary Science Reviews, 109, 38–48, doi:10.1016/j.quascirev.2014.11.012, http://dx.doi.org/10.1016/j.quascirev.2014.11.012, 2015.

Galbraith, E. D. and Martiny, A. C.: A simple nutrient-dependent mechanism for predicting the stoichiometry of marine ecosystems, P. Natl. Acad. Sci. USA, 112, 8199–8204, doi:10.1073/pnas.1423917112, 2015.

Galbraith, E. D., Gnanadesikan, A., Dunne, J. P., and Hiscock, M. R.: Regional impacts of iron-light colimitation in a global biogeochemical model, Biogeosciences, 7, 1043–1064, doi:10.5194/bg-7-1043-2010, 2010.

Galbraith, E. D., Kwon, E. Y., Gnanadesikan, A., Rodgers, K. B., Griffies, S. M., Bianchi, D., Sarmiento, J. L., Dunne, J. P., Simeon, J., Slater, R. D., Wittenberg, A. T., and Held, I. M.: Climate Variability and Radiocarbon in the CM2Mc Earth System Model, J. Climate, 24, 4230–4254, doi:10.1175/2011jcli3919.1, 2011.

Galbraith, E. D., Dunne, J. P., Gnanadesikan, A., Slater, R. D., Sarmiento, J. L., Dufour, C. O., de Souza, G. F., Bianchi, D., Claret, M., Rodgers, K. B., and Marvasti, S. S.: Complex functionality with minimal computation: Promise and pitfalls of reduced-tracer ocean

biogeochemistry models, Journal of Advances in Modeling Earth Systems, 7, 2012–2028, doi:10.1002/2015ms000463, http://dx.doi.org/10.1002/2015MS000463, 2015.

Gebbie, G. and Huybers, P.: How is the ocean filled?, Geophys. Res. Lett., 38, doi:10.1029/2011gl046769, 2011.

Goodwin, P., Follows, M. J., and Williams, R. G.: Analytical relationships between atmospheric carbon dioxide, carbon emissions, and ocean processes, Global Biogeochem. Cy., 22, doi:10.1029/2008gb003184, 2008.

Gruber, N., Sarmiento, J. L., and Stocker, T. F.: An improved method for detecting anthropogenic CO_2 in the oceans, Global Biogeochemical Cycles, 10, 809–837, doi:10.1029/96gb01608, http://dx.doi.org/10.1029/96GB01608, 1996.

Hayes, C. T., Martínez-García, A., Hasenfratz, A. P., Jaccard, S. L., Hodell, D. A., Sigman, D. M., Haug, G. H., and Anderson, R. F.: A stagnation event in the deep South Atlantic during the last interglacial period, Science, 346, 1514–1517, doi:10.1126/science.1256620, 2014.

IPCC: Climate Change 2007: The Physical Science Basis. Contribution of Working Group I to the Fourth Assessment Report of the Intergovernmental Panel on Climate Change, Cambridge University Press, Cambridge, United Kingdom, 2007.

Ito, T. and Follows, M. J.: Preformed phosphate, soft tissue pump and atmospheric CO_2, J. Mar. Res., 63, 813–839, doi:10.1357/0022240054663231, 2005.

Ito, T. and Follows, M. J.: Air-sea disequilibrium of carbon dioxide enhances the biological carbon sequestration in the Southern Ocean, Global Biogeochem. Cy., 27, 1129–1138, doi:10.1002/2013gb004682, 2013.

Ito, T., Follows, M. J., and Boyle, E. A.: Is AOU a good measure of respiration in the oceans?, Geophys. Res. Lett., 31, doi:10.1029/2004GL020900, 2004.

Jaccard, S. L., Galbraith, E. D., Martínez-García, A., and Anderson, R. F.: Covariation of deep Southern Ocean oxygen and atmospheric CO_2 through the last ice age, Nature, 530, 207–210, doi:10.1038/nature16514, 2016.

Kohfeld, K. E. and Ridgwell, A.: Glacial-interglacial variability in atmospheric CO_2, Geophysical Monograph Series, pp. 251–286, doi:10.1029/2008gm000845, 2009.

Köhler, P. and Fischer, H.: Simulating low frequency changes in atmospheric CO_2 during the last 740 000 years, Clim. Past, 2, 57–78, doi:10.5194/cp-2-57-2006, http://dx.doi.org/10.5194/cp-2-57-2006, 2006.

Kwon, E. Y., Primeau, F., and Sarmiento, J. L.: The impact of remineralization depth on the air-sea carbon balance, Nat. Geosci., 2, 630–635, doi:10.1038/NGEO612, 2009.

Laskar, J., Robutel, P., Joutel, F., Gastineau, M., Correia, A. C. M., and Levrard, B.: A long-term numerical solution for the insolation quantities of the Earth, Astron. Astrophys., 428, 261–285, doi:10.1051/0004-6361:20041335, 2004.

Le Quéré, C., Rödenbeck, C., Buitenhuis, E. T., Conway, T. J., Langenfelds, R., Gomez, A., Labuschagne, C., Ramonet, M., Nakazawa, T., Metzl, N., Gillett, N., and Heimann, M.: Saturation of the Southern Ocean CO_2 Sink Due to Recent Climate Change, Science, 316, 1735–1738, doi:10.1126/science.1136188, http://dx.doi.org/10.1126/science.1136188, 2007.

Lu, Z., Hoogakker, B. A. A., Hillenbrand, C.-D., Zhou, X., Thomas, E., Gutchess, K. M., Lu, W., Jones, L., and Rickaby, R. E. M.: Oxygen depletion recorded in upper waters of the glacial Southern Ocean, Nat. Commun., 7, doi:10.1038/ncomms11146, 2015.

Mahowald, N. M., Muhs, D. R., Levis, S., Rasch, P. J., Yoshioka, M., Zender, C. S., and Luo, C.: Change in atmospheric mineral aerosols in response to climate: Last glacial period, preindustrial, modern, and doubled carbon dioxide climates, Journal of Geophysical Research: Atmospheres, 111, doi:10.1029/2005JD006653, http://dx.doi.org/10.1029/2005JD006653, d10202, 2006.

Marinov, I., Follows, M., Gnanadesikan, A., Sarmiento, J. L., and Slater, R. D.: How does ocean biology affect atmospheric pCO_2? Theory and models, J. Geophys. Res., 113, doi:10.1029/2007jc004598, 2008a.

Marinov, I., Gnanadesikan, A., Sarmiento, J. L., Toggweiler, J. R., Follows, M., and Mignone, B. K.: Impact of oceanic circulation on biological carbon storage in the ocean and atmospheric pCO_2, Global Biogeochem. Cy., 22, doi:10.1029/2007gb002958, 2008b.

Martin, J. H.: Glacial-interglacial CO_2 change: The Iron Hypothesis, Paleoceanography, 5, 1–13, doi:10.1029/pa005i001p00001, 1990.

Martin, J. H., Knauer, G. A., Karl, D. M., and Broenkow, W. W.: VERTEX: carbon cycling in the northeast Pacific, Deep-Sea Res. A, 34, 267–285, doi:10.1016/0198-0149(87)90086-0, 1987.

Martiny, A. C., Vrugt, J. A., Primeau, F. W., and Lomas, M. W.: Regional variation in the particulate organic carbon to nitrogen ratio in the surface ocean, Global Biogeochem. Cy., 27, 723–731, doi:10.1002/gbc.20061, 2013.

Matsumoto, K., Hashioka, T., and Yamanaka, Y.: Effect of temperature-dependent organic carbon decay on atmospheric pCO_2, J. Geophys. Res., 112, doi:10.1029/2006JG000187, 2007.

Moore, C. M., Mills, M. M., Arrigo, K. R., Berman-Frank, I., Bopp, L., Boyd, P. W., Galbraith, E. D., Geider, R. J., Guieu, C., Jaccard, S. L., Jickells, T. D., La Roche, J., Lenton, T. M., Mahowald, N. M., Marañón, E., Marinov, I., Moore, J. K., Nakatsuka, T., Oschilles, A., Saito, M. A., Thingstad, T. F., Tsuda, A., and Ulloa, O.: Processes and patterns of oceanic nutrient limitation, Nature Geoscience, 6, 701–710, doi:10.1038/ngeo1765, http://dx.doi.org/10.1038/ngeo1765, 2013.

Myhre, G., Highwood, E. J., Shine, K. P., and Stordal, F.: New estimates of radiative forcing due to well mixed greenhouse gases, Geophysical Research Letters, 25, 2715–2718, doi:10.1029/98GL01908, http://dx.doi.org/10.1029/98GL01908, 1998.

Nickelsen, L. and Oschlies, A.: Enhanced sensitivity of oceanic CO_2 uptake to dust deposition by iron-light colimitation, Geophys. Res. Lett., 42, 492–499, doi:10.1002/2014gl062969, 2015.

Ödalen, J. N., Oliver, K. I. C., Brodeau, L., and Ridgwell, A.: The influence of the ocean circulation state on ocean carbon storage and CO_2 drawdown potential in an Earth system model, Biogeosciences, 15, 1367–1393, doi:10.5194/bg-15-1367-2018, 2018.

Parekh, P., Dutkiewicz, S., Follows, M. J., and Ito, T.: Atmospheric carbon dioxide in a less dusty world, Geophys. Res. Lett., 33, doi:10.1029/2005gl025098, 2006.

Piotrowski, A. M., Goldstein, S. L., Hemming, S. R., and Fairbanks, R. G.: Temporal Relationships of Carbon Cycling and Ocean Circulation at Glacial Boundaries, Science, 307, 1933–1938, doi:10.1126/science.1104883, 2005.

Roth, R., Ritz, S. P., and Joos, F.: Burial-nutrient feedbacks amplify the sensitivity of atmospheric carbon dioxide to changes in organic matter remineralisation, Earth System Dynamics, 5, 321–343, doi:10.5194/esd-5-321-2014, 2014.

Russell, J. L. and Dickson, A. G.: Variability in oxygen and nutrients in South Pacific Antarctic Intermediate Water, Global Biogeochem. Cy., 17, doi:10.1029/2000GB001317, 2003.

Schmittner, A. and Galbraith, E. D.: Glacial greenhouse-gas fluctuations controlled by ocean circulation changes, Nature, 456, 373–376, doi:10.1038/nature07531, 2008.

Sigman, D. M. and Boyle, E. A.: Glacial/interglacial variations in atmospheric carbon dioxide, Nature, 407, 859–869, doi:10.1038/35038000, http://dx.doi.org/10.1038/35038000, 2000.

Sigman, D. M., Hain, M. P., and Haug, G. H.: The polar ocean and glacial cycles in atmospheric CO_2 concentration, Nature, 466, 47–55, doi:10.1038/nature09149, 2010.

Skinner, L. C.: Glacial-interglacial atmospheric CO_2 change: a possible "standing volume" effect on deep-ocean carbon sequestration, Clim. Past, 5, 537–550, doi:10.5194/cp-5-537-2009, http://dx.doi.org/10.5194/cp-5-537-2009, 2009.

Stephens, B. B. and Keeling, R. F.: The influence of Antarctic sea ice on glacial-interglacial CO_2 variations, Nature, 404, 171–174, doi:10.1038/35004556, 2000.

Tagliabue, A., Aumont, O., DeAth, R., Dunne, J. P., Dutkiewicz, S., Galbraith, E., Misumi, K., Moore, J. K., Ridgwell, A., Sherman, E., Stock, C., Vichi, M., Völker, C., and Yool, A.: How well do global ocean biogeochemistry models simulate dissolved iron distributions?, Global Biogeochem. Cy., 30, 149–174, doi:10.1002/2015GB005289, 2016.

Takahashi, T. Sutherland, S. C., Wanninkhof, R., Sweeney, C., Feely, R. A., Chipman, D. W., Hales, B., Friederich, G., Chavez, F., Watson, A., Bakker, D. C. E., Schuster, U., Metzl, N., Yoshikawa-Inoue, H., Ishii, M., Midorikawa, T., Nojiri, Y., Sabine, C., Olafsson, J., Arnarson, T. S., Tilbrook, B., Johannessen, T., Olsen, A., Bellerby, R., Körtzinger, A., Steinhoff, T., Hoppema, M., de Baar, H. J. W., Wong, C. S., Delille, B., and Bates, N. R.: Climatological mean and decadal changes in surface ocean pCO_2, and net sea-air CO_2 flux over the global oceans, Deep-Sea Res. II, 56, 554–577, doi:10.1016/j.dsr2.2008.12.009, 2009.

Toggweiler, J. R., Murnane, R., Carson, S., Gnanadesikan, A., and Sarmiento, J. L.: Representation of the carbon cycle in box models and GCMs: 2. Organic pump, Global Biogeochem. Cy., 17, doi:10.1029/2001gb001841, 2003.

Tschumi, T., Joos, F., Gehlen, M., and Heinze, C.: Deep ocean ventilation, carbon isotopes, marine sedimentation and the deglacial CO_2 rise, Clim. Past, 7, 771–800, doi:10.5194/cp-7-771-2011, 2011.

Volk, T. and Hoffert, M. I.: The Carbon Cycle and Atmospheric CO_2: Natural Variations Archean to Present, chap. Ocean Carbon Pumps: Analysis of Relative Strengths and Efficiencies in Ocean-Driven Atmospheric CO_2 Changes, pp. 99–110, American Geophysical Union, doi:10.1029/GM032p0099, http://dx.doi.org/10.1029/GM032p0099, 1985.

Watson, A. J., Vallis, G. K., and Nikurashin, M.: Southern Ocean buoyancy forcing of ocean ventilation and glacial atmospheric CO_2, Nature Geoscience, 8, 861–865, doi:10.1038/ngeo2538, http://dx.doi.org/10.1038/ngeo2538, 2015.

Williams, R. G. and Follows, M. J.: Ocean Dynamics and the Carbon Cycle: Principles and Mechanisms, Cambridge University Press, 2011.

Zeebe, R. E. and Wolf-Gladrow, D.: CO_2 in Seawater: Equilibrium, Kinetics, Isotopes, vol. 65, Elsevier Oceanography Series, Amsterdam, 2001.

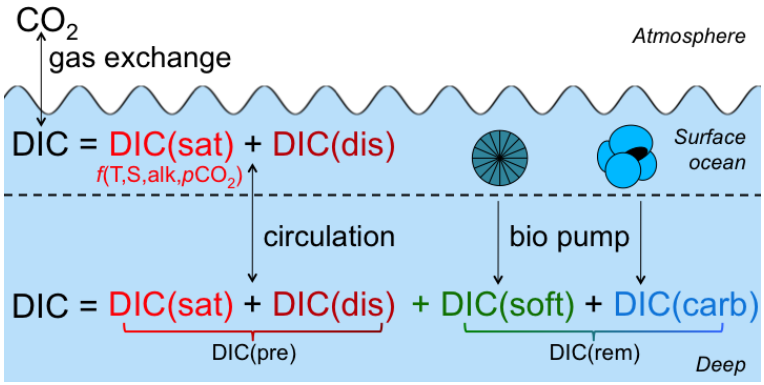

Figure 1. ~~Global average~~ Illustration of the decomposition framework used for DIC in this paper. In the surface ocean, DIC is equal to $DIC_{pre} = DIC_{sat} + DIC_{dis}$. Carbon taken up by biology in the surface ocean sinks and ~~separate components~~ remineralizes in ~~simulations 1-36 as~~ the water column to add two additional components at depths: $DIC_{rem} = DIC_{soft} + DIC_{carb}$.

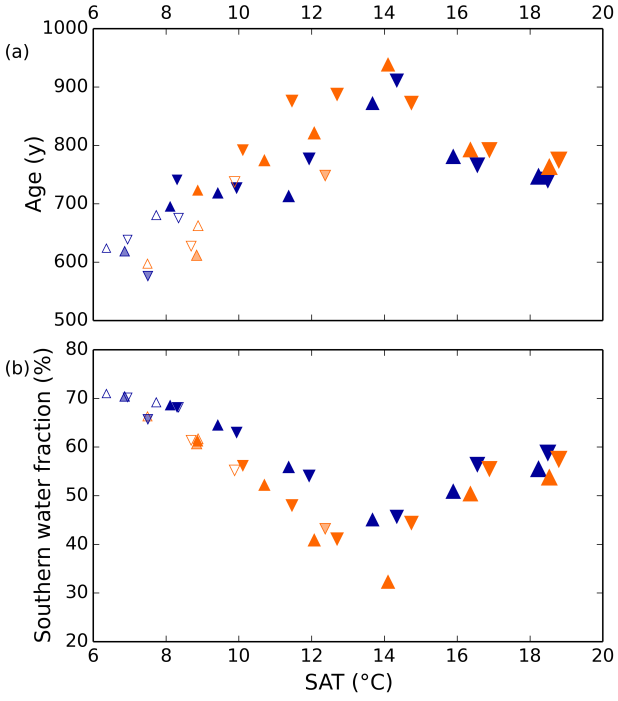

Figure 2. Global ocean ventilation and proportion of southern-sourced deepwater. (a~~function~~) The global ocean average ideal age (low age corresponds to high ventilation) and (b) the fraction of ~~CO_2~~water in the global ocean originating from the surface south of 30^{o}S are anti-correlated over the range of SAT in these model runs. Orange and blue symbols represent high and low obliquity scenarios, respectively; triangles pointing upward and downward represent greater northern and southern hemisphere seasonality or precession 270^o and 90^o, respectively; outlines are scenarios with LGM ice sheets; light shading indicates scenarios with LGM ice sheet topography but PI albedo. The size of the symbols corresponds to the SAT.

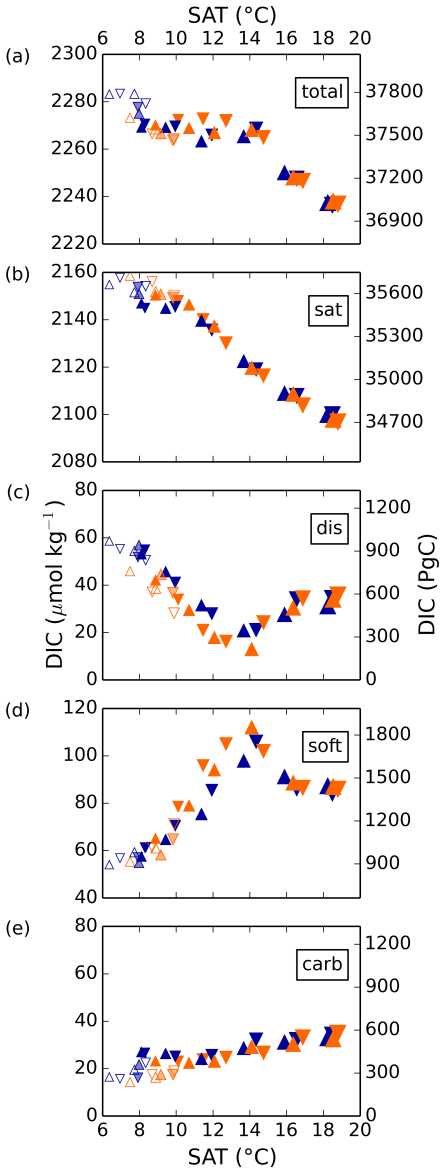

Figure 3. ~~Changes in total global~~ Global average DIC and ~~each of the~~ separate components ~~(iron fertilization simulation minus associated control run). Simulations were either run under pre-industrial or glacial-like conditions (~~in ~~the case~~ simulations 1-36 as a function of ~~the latter~~surface air temperature. Orange and blue symbols represent high and low obliquity scenarios, ~~results~~ respectively; triangles pointing upward and downward represent ~~the average of four runs at $CO_2 = 180$ ppm~~ greater northern and southern hemisphere seasonality or precession 270° and 90°, respectively; outlines are scenarios with LGM ice sheets~~), as well as 100% and 75% of the default remineralization rate of organic matter. The close agreement of the left and middle panels~~ ; light shading indicates ~~that the effects of iron fertilization and changes in the remineralization rate are linearly additive in this model~~scenarios with LGM ice sheet topography but PI albedo.

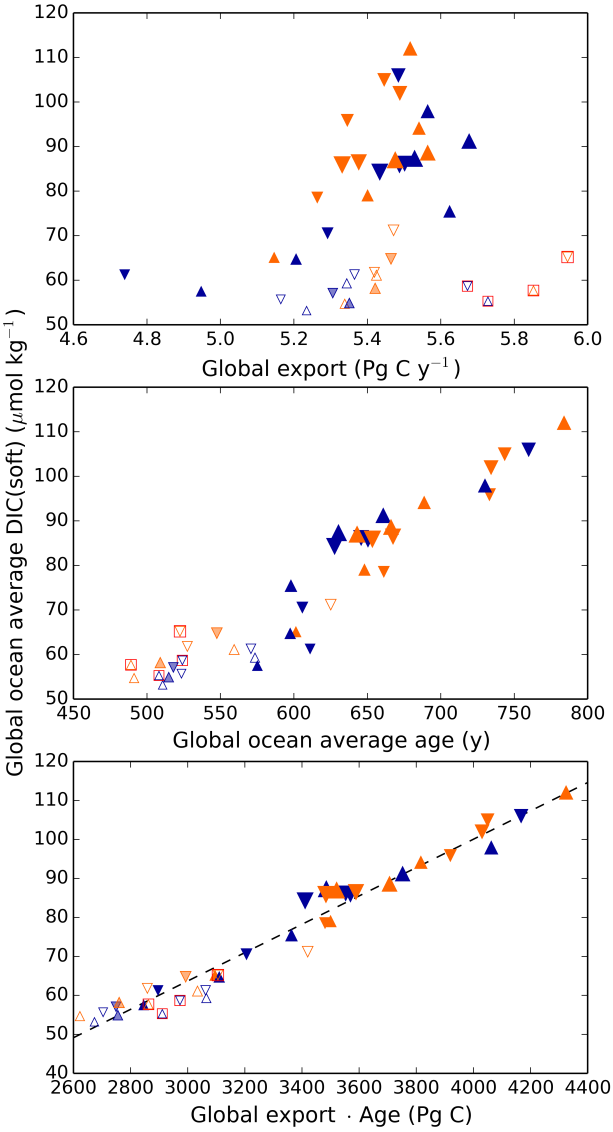

Figure 4. Globally averaged DIC_{soft}, or remineralized carbon from the soft tissue pump, can be approximated remarkably well by the global export flux of organic carbon at 100 m multiplied by the average age of the ocean. The latter is an ideal age tracer in the model that is set to 0 at the surface and ages by 1 y each model year in the ocean interior. ~~Markers as in fig. 3~~ Orange and blue symbols represent high and low obliquity scenarios, respectively; triangles pointing upward and downward represent greater northern and southern hemisphere seasonality or precession 270° and 90°, respectively; outlines are scenarios with ~~the~~ LGM ice sheets; light shading indicates scenarios with LGM ice sheet topography but PI albedo. Red boxes indicate Fe fertlization simulations (runs 37 – 40). The size of the symbols ~~corresponding~~ corresponds to the ~~CO_2 level~~SAT.

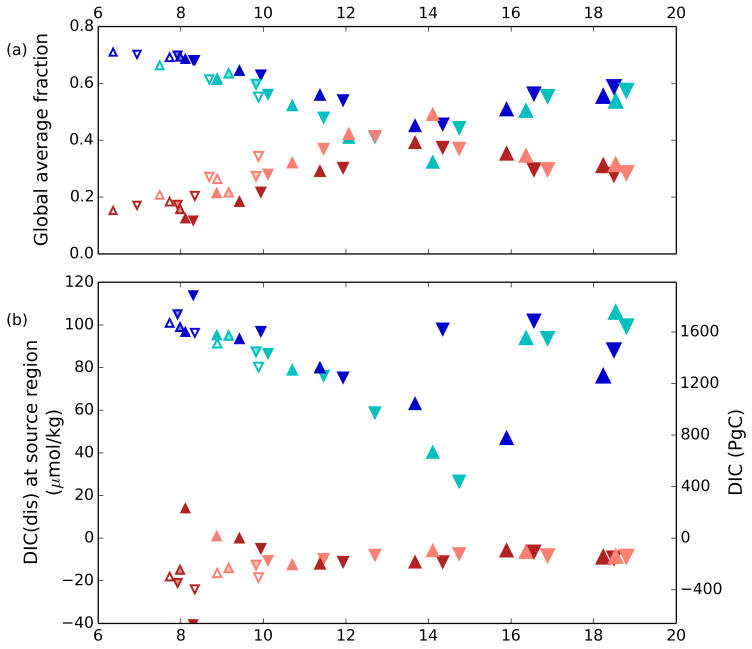

Figure 5. (a) Global average fraction of northern- (reddish colors) and southern-sourced (bluish colors) water. (b) ~~Average~~ Annual average values of DIC_{dis} of these water masses determined at ~~100~~ 25 m depth in the model during model years and at locations where deep convection ~~down to 200 m~~ occurs. ~~Markers are identical to fig. 3 with lighter colors representing high~~ Pink and ~~darker colors~~ cyan (red and blue) symbols represent high (low) obliquity scenarios; triangles pointing upward and downward represent greater northern and southern hemisphere seasonality or precession 270° and 90°, respectively; outlines are scenarios with LGM ice sheets; light shading indicates scenarios with LGM ice sheet topography but PI albedo. The size of the symbols corresponds to the SAT.

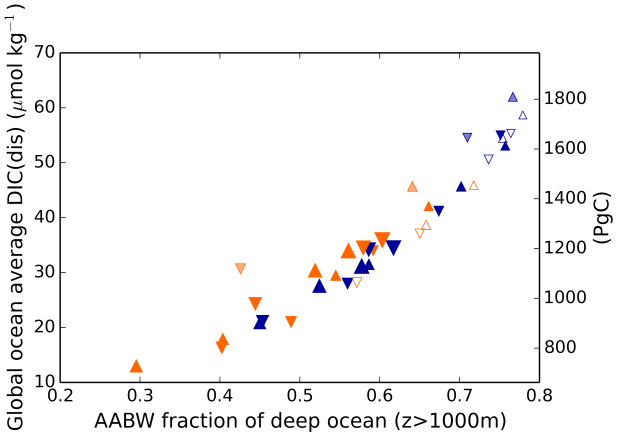

Figure 6. Global average DIC_{dis} as a function of the fraction of the ocean below ~~500 m~~ 1 km derived from the surface Southern Ocean~~; symbols as in fig~~. ~~3~~ Orange and blue symbols represent high and low obliquity scenarios, respectively; triangles pointing upward and downward represent greater northern and southern hemisphere seasonality or precession 270^o and 90^o, respectively; outlines are scenarios with ~~the~~ LGM ice sheets; light shading indicates scenarios with LGM ice sheet topography but PI albedo. The size of the symbols ~~corresponding~~ corresponds to the ~~CO_2 level~~SAT.

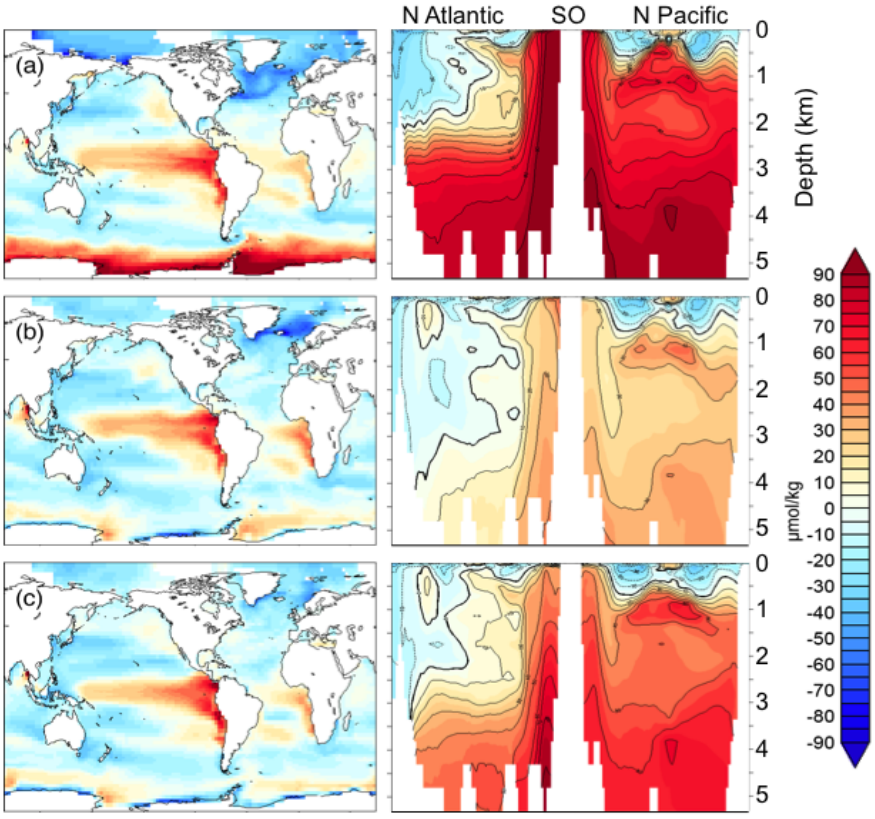

~~Zonally averaged~~ HW (~~a~~see section 2.2)~~DIC flux to~~ . Depth transects represent the ~~atmosphere; North~~ Atlantic (~~b~~left) ~~O_2 flux to the atmosphere; -~~ Southern Ocean (~~e~~center) ~~surface ocean DIC_{dis}; -~~ North Pacific (~~d~~right)~~surface ocean $O_{2_{dis}}$~~.~~Results from three simulations are shown: glacial (black); interglacial (red); CO_2 = 911 (green). Fractional sea ice cover (0 - 100%) is shown in each plot as a reference.~~

~~Zonally averaged~~ HW (~~a~~see section 2.2)~~DIC flux to~~ . Depth transects represent the ~~atmosphere; North~~ Atlantic (~~b~~left) ~~O_2 flux to the atmosphere; -~~ Southern Ocean (~~e~~center) ~~surface ocean DIC_{dis}; -~~ North Pacific (~~d~~right)~~surface ocean $O_{2_{dis}}$~~.~~Results from three simulations are shown: glacial (black); interglacial (red); CO_2 = 911 (green). Fractional sea ice cover (0 - 100%) is shown in each plot as a reference.~~

Figure 7. ~~Surface ocean~~ DIC_{dis} ~~and annually averaged sea ice cover~~ (~~contours showing 20% intervals~~μmol kg^{-1}) ~~in~~ for simulations ~~emulating the following states:~~ (a) ~~glacial~~CW; (b) ~~interglacial~~MW; (c) ~~CO_2 = 911.~~

~~Zonally averaged~~ HW (~~a~~see section 2.2)~~DIC flux to~~ . Depth transects represent the ~~atmosphere; North~~ Atlantic (~~b~~left) ~~O_2 flux to the atmosphere; -~~ Southern Ocean (~~e~~center) ~~surface ocean DIC_{dis}; -~~ North Pacific (~~d~~right)~~surface ocean $O_{2_{dis}}$~~.~~Results from three simulations are shown: glacial (black); interglacial (red); CO_2 = 911 (green). Fractional sea ice cover (0 - 100%) is shown in each plot as a reference.~~

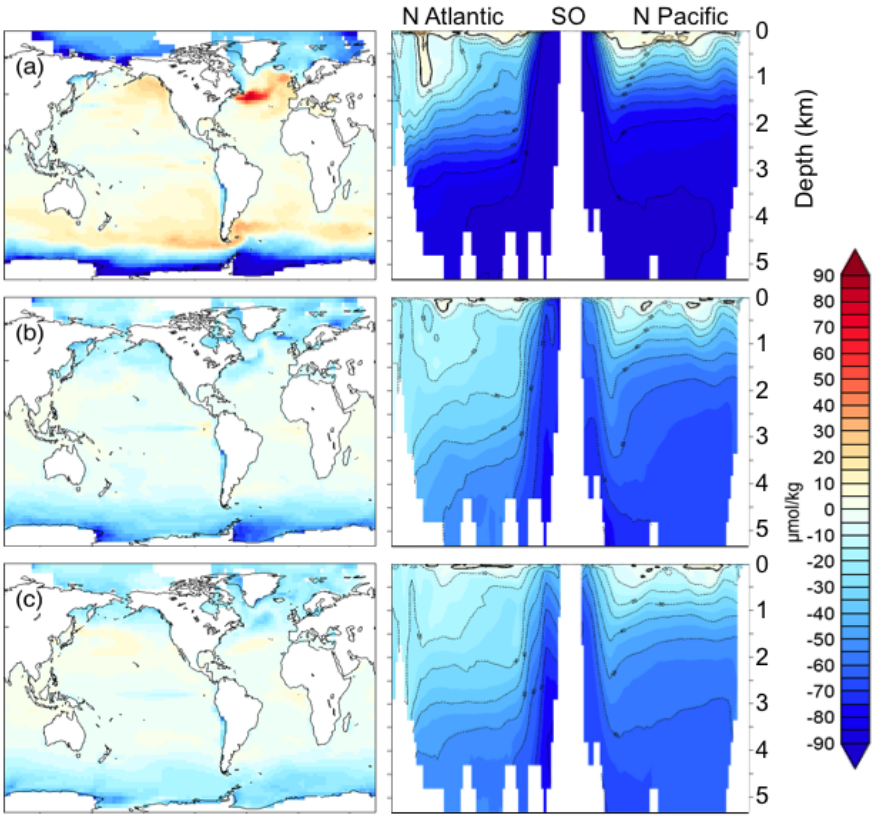

Figure 8. ~~DIC$_{dis}$~~ $O_{2_{dis}}$ (μmol kg^{-1}) for simulations (a) ~~glacial~~CW; (b) ~~interglacial~~MW; (c) ~~CO_2 = 911~~HW (see section 2.2). Depth transects represent the North Atlantic (left) - Southern Ocean (center) - North Pacific (right).

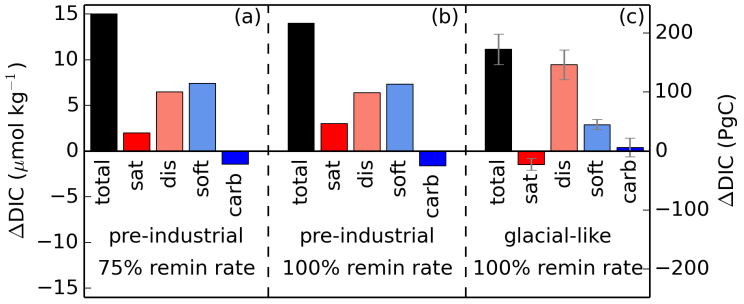

~~Using globally averaged NO_3 and~~ . Simulations were either run under pre-industrial or glacial-like conditions (in the ~~NO_3 denitrification sink~~ case of the latter, results represent the average of the four GL runs, with error bars showing the standard deviation within the four runs), as well as ~~values of NO_{3pre}~~ 100% and ~~DIC_{dis} in regions~~ 75% of ~~deepwater formation in~~ the ~~Southern Ocean~~ default remineralization rate of organic matter. The close agreement of the left and middle panels indicates that the ~~North Atlantic weighted by the fractions~~ effects of iron fertilization and changes in the ~~world oceans derived from each~~ remineralization rate are approximately linearly additive in this model.

~~Using globally averaged NO_3 and~~ . Simulations were either run under pre-industrial or glacial-like conditions (in the ~~NO_3 denitrification sink~~ case of the latter, results represent the average of the four GL runs, with error bars showing the standard deviation within the four runs), as well as ~~values of NO_{3pre}~~ 100% and ~~DIC_{dis} in regions~~ 75% of ~~deepwater formation in~~ the ~~Southern Ocean~~ default remineralization rate of organic matter. The close agreement of the left and middle panels indicates that the ~~North Atlantic weighted by the fractions~~ effects of iron fertilization and changes in the ~~world oceans derived from each~~ remineralization rate are approximately linearly additive in this model.

Figure 9. ~~As~~ Iron-fertilized changes in ~~fig. A for O_{2dis}~~ total global average DIC and each of the components (~~μmol kg^{-1}~~ iron fertilization simulation minus associated control run)

~~Using globally averaged NO_3 and~~ . Simulations were either run under pre-industrial or glacial-like conditions (in the ~~NO_3 denitrification sink~~ case of the latter, results represent the average of the four GL runs, with error bars showing the standard deviation within the four runs), as well as ~~values of NO_{3pre}~~ 100% and ~~DIC_{dis} in regions~~ 75% of ~~deepwater formation in~~ the ~~Southern Ocean~~ default remineralization rate of organic matter. The close agreement of the left and middle panels indicates that the ~~North Atlantic weighted by the fractions~~ effects of iron fertilization and changes in the ~~world oceans derived from each~~ remineralization rate are approximately linearly additive in this model.

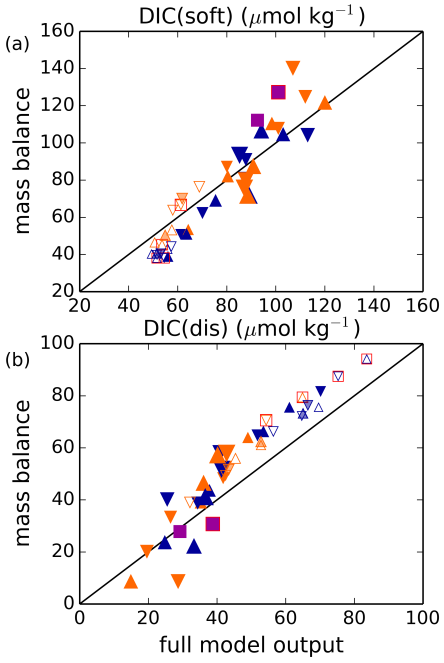

Figure 10. Simple parametrization of ~~these sites~~global DIC_{dis} and DIC_{soft} from water mass characteristics. Following eq. 12 for (a) DIC_{soft} and (b) DIC_{dis} separately, ~~it is possible to reconstruct~~ this model shows that the sum of the ~~globally averaged~~ global average $DIC_{~~dis~~ soft}$ and $DIC_{~~soft:~~}$

$$DIC_{dis_{global}} + DIC_{soft_{global}} \approx r_{C:N} \cdot (NO_{3_{global}} + NO_{3_{den,global}}) + \sum_{i=1}^{n} f_i \cdot (DIC_{dis_i} - r_{C:N} \cdot NO_{3_{pre_i}})$$

$_{dis}$ at steady-state can be estimated fairly robustly as the result of a simple mass balance of the relevant parameters in the most important ventilating water masses. Here, we take into account upper-ocean water masses (above 1 km) formed in the North Pacific, North Atlantic, and Southern Ocean, ~~as well as~~ and deep water masses formed in the North Atlantic and Southern Ocean. In each plot, the full model output is shown on the x-axis and the result of the mass balance approximation on the y-axis. ~~Markers as in fig. 3~~ Orange and blue symbols represent high and low obliquity scenarios, respectively; triangles pointing upward and downward represent greater northern and southern hemisphere seasonality or precession 270° and 90°, respectively; outlines are scenarios with ~~the~~ LGM ice sheets; light shading indicates scenarios with LGM ice sheet topography but PI albedo. The size of the symbols ~~corresponding~~ corresponds to the ~~CO_2 level~~SAT. The purple ~~squares~~ square represents the pre-industrial ~~simulations~~ simulation (~~runs~~ run 41~~–42~~), and ~~a~~ red ~~square around the symbol indicates~~ boxes indicate Fe fertlization simulations (runs ~~with iron fertilization~~37 – 40).

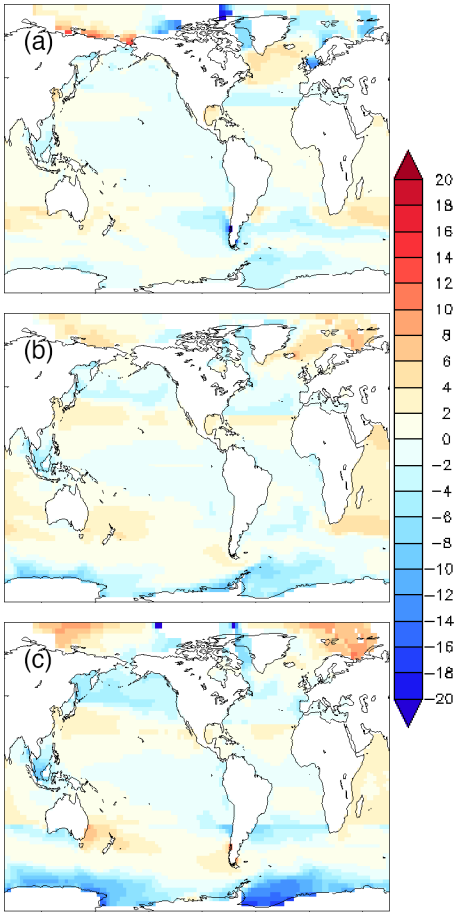

Figure A1. Shown is the difference between the exact DIC_{dis} surface field in μmol kg^{-1}, where DIC_{sat} has been calculated using the surface alkalinity ($alk[z=0] = alk_{pre}[z=0]$) and $DIC_{soft}[z=0] = DIC_{carb}[z=0] = 0$. Differences are shown for (a) ~~glacial~~LGM; (b) ~~interglacial~~PI; (c) ~~CO_2 = 911~~WF.

Table 1. Simulation overview. A total of 44 simulations were analyzed with varying ~~CO_2~~ radiative forcing (RF), obliquity, precession, ice sheets (PI = pre-industrial; LGM = Last Glacial Maximum reconstruction; LGM* = topography of LGM ice sheets but with PI albedo), and with and without iron fertilization. Runs 1 – 40 are described by Galbraith and de Lavergne (2018). Runs 43 and 44 and identical to 41 and 42 but the remineralization rate of sinking organic matter is reduced by 25%.

run	**RF in pCO_2 equivalents (ppm)**	**obliquity**	**precession**	**IS**	**Fe**	**remin**
1-24	180, 220, 270, 405, 607, 911	22°, 24.5°	90°, 270°	PI		
25-28	220	22°, 24.5°	90°, 270°	LGM		
29-32	180	22°, 24.5°	90°, 270°	LGM*		
33-36	180	22°, 24.5°	90°, 270°	LGM		
37-40	180	22°, 24.5°	90°, 270°	LGM	X	
41	270	23.4°	102.9°	PI		
42	270	23.4°	102.9°	PI	X	
43	270	23.4°	102.9°	PI		75%
44	270	23.4°	102.9°	PI	X	75%